

## TI Designs: TIDA-01377

# 誘導性センシングを使用したケース不正開封検出のリファレンス・デザイン



### 概要

スマート・メータを囲む物理的なケースは、改変に対する最初の防御線です。スマート・メータには、メータのケースが開かれたことを検出し、改変攻撃の可能性をサービス・プロバイダへ警告する方法を組み込む必要があります。TIDA-01377リファレンス・デザインでは、小さな誘導性センサを使用して、メータのケースが開かれたかどうかを正確に、高い信頼性で判定し、このような改変を検出する、低消費電力の新しい検出方法を実装します。この新しいソリューションでは、時間とともに消耗する機械式部品が不要になり、システムの信頼性が向上します。このシステムはスマート電力メータに実装されますが、この設計技法は水道、ガス、熱量メータにも応用できます。

### リソース

[TIDA-01377](#)

[LDC0851](#)

[MSP430F67791A](#)

[デザイン・フォルダ](#)

[プロダクト・フォルダ](#)

[プロダクト・フォルダ](#)

### 特長

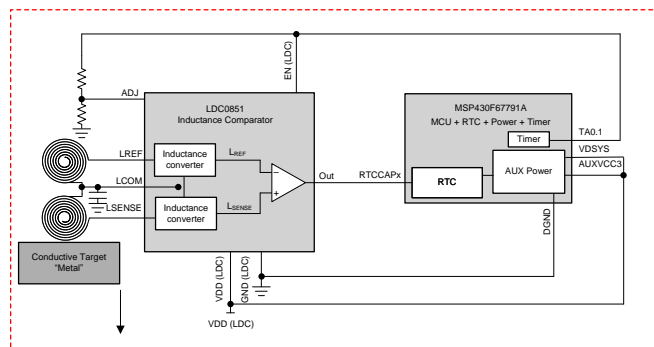
- ケース不正開封イベントの非接触式検出
- 最小4mmのケース移動を正確に検出
- 単一の誘導性センサにより、端末ブロック・カバーおよびメイン・カバーの開封を検出
- 1Hzのサンプリング時に、消費電流は約2μA
- DC磁気改変への耐性

### アプリケーション

- [電気メータ](#)
- [ガス・メータ](#)
- [水道メータ](#)
- [熱量メータ](#)



[E2Eエキスパートに質問](#)





使用許可、知的財産、その他免責事項は、最終ページにあるIMPORTANT NOTICE(重要な注意事項)をご参照くださいますようお願いいたします。英語版のTI製品についての情報を翻訳したこの資料は、製品の概要を確認する目的で便宜的に提供しているものです。該当する正式な英語版の最新情報は、[www.ti.com](http://www.ti.com)で閲覧でき、その内容が常に優先されます。TIでは翻訳の正確性および妥当性につきましては一切保証いたしません。実際の設計などの前には、必ず最新版の英語版をご参照くださいますようお願いいたします。

## 1 System Description

Each year utility providers lose billions of dollars in revenue due to non-technical losses. One form of non-technical loss is meter tampering where individuals attempt to stop or slow down the accumulation of consumption statistics. To combat meter tampering, many smart meters have anti-tamper mechanisms that detect and harden a meter against tampering. The first line of defense against meter tampering is the physical case. To reinforce this line of protection, meters commonly have some form of integrated intrusion detection subsystem to detect the opening of the case.

Historically, a mechanical solution has been used to detect a case open event. One such solution uses a button which is compressed by the top of the case when assembled. If the case is opened the button is released and the host microcontroller (MCU) is notified. A few limitations to the mechanical case tampering implementation exist. First, there are issues with long-term stability of the mechanical implementation because the push-buttons can get stuck, thereby paralyzing the functionality of the case tamper detection. To mitigate these issues, higher reliability switches can be used; however, these highly-reliable switches increase the system cost. In addition, there are ways to tamper with this mechanism so that the system can be tricked to think that the case is closed when it is open and a single button may not detect the case being opened across multiple points around the meter perimeter.

This design implements a more reliable solid-state method to detect case open events based upon inductive sensing of the movement of a metal target. The LDC0851 differentially-compensated inductive switch provides highly-accurate sensing of the opening of the case independent of any component aging or environmental factors such as temperature, humidity, or the presence of contaminants such as dirt or oil. Inductive sensing is also immune to the effects of DC magnets, countering another common type of meter tampering (discussed in the [TIDA-00839 reference design \[1\]](#)). An LDC0851-based design allows sensing across multiple points on the meter perimeter through the implementation of multiple sensing coils on the main printed-circuit board (PCB) and with only a single LDC0851 switch.

Multiple sensor coil implementations are possible to customize the system to a specific meter case form factor. In a two-cover meter design, one coil can sense openings in the main case while a second detects an opening of the terminal block cover. Alternatively, coils can be placed on opposite PCB corners to maximize sense coverage around the meter perimeter. The primary external components required by the LDC0851 for sensing are a target metal plus reference and sense inductors, each of which can be fabricated as coils on the meter PCB.

In addition to the LDC0851, this design also uses a MSP430F67791A MCU that has an internal real-time clock (RTC) with capture pins that log the time of case tampering. This MCU also provides the pulses that are used to enable and disable the LDC0851 device to reduce the current consumption. This design samples the sensor at a 1-Hz rate, lowering the average current consumption to approximately 2  $\mu$ A. In addition to providing the enable pulses, the MCU also provides the power source for the LDC0851 device. This power source has support for backup power sources so that the LDC0851 can effectively be powered from mains when it is available and automatically switch to a backup power source when it is not available.

In this design, the functionality of the case tamper detection is implemented with an electricity meter case. The techniques used in this design are also applicable to other types of smart meters for water, gas, and heat measurement. Two different PCBs are associated with this design. The first PCB is associated with a one-sense-coil implementation that is used to detect when the terminal block cover has been opened. The second PCB is associated with a two-sense-coil implementation that is used to detect when the terminal block cover is opened as well as when the main cover is opened.

## 1.1 Key System Specifications

表 1. Key System Specifications

PARAMETER	SPECIFICATIONS	DETAILS
Case tamper detection implementation	Inductive	<a href="#">3.1</a>
Meter case type	Three-phase electricity meter (extendable to other cases or other meter types)	<a href="#">3.3.4.1.1</a>
Case tamper detection location, one-sense-coil implementation	Terminal block cover	<a href="#">3.3.4.1.1</a>
Case tamper detection location, two-sense-coil implementation	Terminal block cover and main cover	<a href="#">3.3.4.2.1</a>
Target metal utilized	Copper tape	<a href="#">3.4</a>
Sense and reference coil diameter	25 mm	<a href="#">3.3</a>
Sense and reference coil trace width	10 mil	<a href="#">3.3</a>
Sense and reference coil spacing between traces	10 mil	<a href="#">3.3</a>
Number of PCB layers for sense coil	Two layers	<a href="#">3.3</a>
Minimum target metal to sense coil distance, one-sense-coil implementation	≈7 mm	<a href="#">3.3.4.1.1</a>
Target metal to sense coil turn ON distance, one-sense-coil implementation	≈7.5 mm	<a href="#">3.3</a>
Target metal to sense coil turn OFF distance, one-sense-coil implementation	≈7.99 mm	<a href="#">3.3</a>
Maximum target metal to sense coil distance, one-sense-coil implementation	≈10 mm	<a href="#">3.3.4.1.1</a>
Change in terminal block cover position to trigger tampering, one-sense-coil implementation	≈0.99 mm	<a href="#">3.3</a>
Sample rate of LDC0851	1 Hz	<a href="#">3.5.2</a>
LDC0851 average current consumption	≈ 2 μA	<a href="#">3.5.2</a>

## 2 System Overview

### 2.1 Block Diagram

In this design, the LDC0851 compares the sense inductance that is between its LSENSE and LCOM pin with the reference inductance that is between its LREF and LCOM pin. False triggers due to environmental factors such as temperature variation or humidity effects are prevented by comparing the reference and sense inductances and matching their free space inductances.

The inductors connected to the LDC0851 pins are implemented as coils on the design PCB. By bringing a conductive target metal near the top of one of these coils driven by the LDC0851, the inductance of the coil decreases, which can be used to cause the output of the LDC0851 to switch states. The LDC0851 output changes based on whether the reference inductance or sense inductance is smaller. For stable output switching, hysteresis is included in the inductance comparisons.

To change the switching point of the LDC0851, the LDC0851 has a threshold adjust feature where an offset can be subtracted from the reference coil inductance measurement. There are 16 offset options (including basic operation mode when no offset is subtracted) where the selected offset value is programmed by applying a certain voltage to the ADJ pin of the LDC0851. If the sense inductance is less than the adjusted reference inductance minus the hysteresis quantity, the output of the LDC0851 is asserted low. If the offset of the sense coil is larger than the adjusted reference coil inductance plus the hysteresis quantity, the output is asserted high.

This design has two variants. The first variant is a one-sense-coil implementation that detects when the terminal block cover of a meter has been opened. [Figure 1](#) shows the block diagram of this one-sense-coil variant.

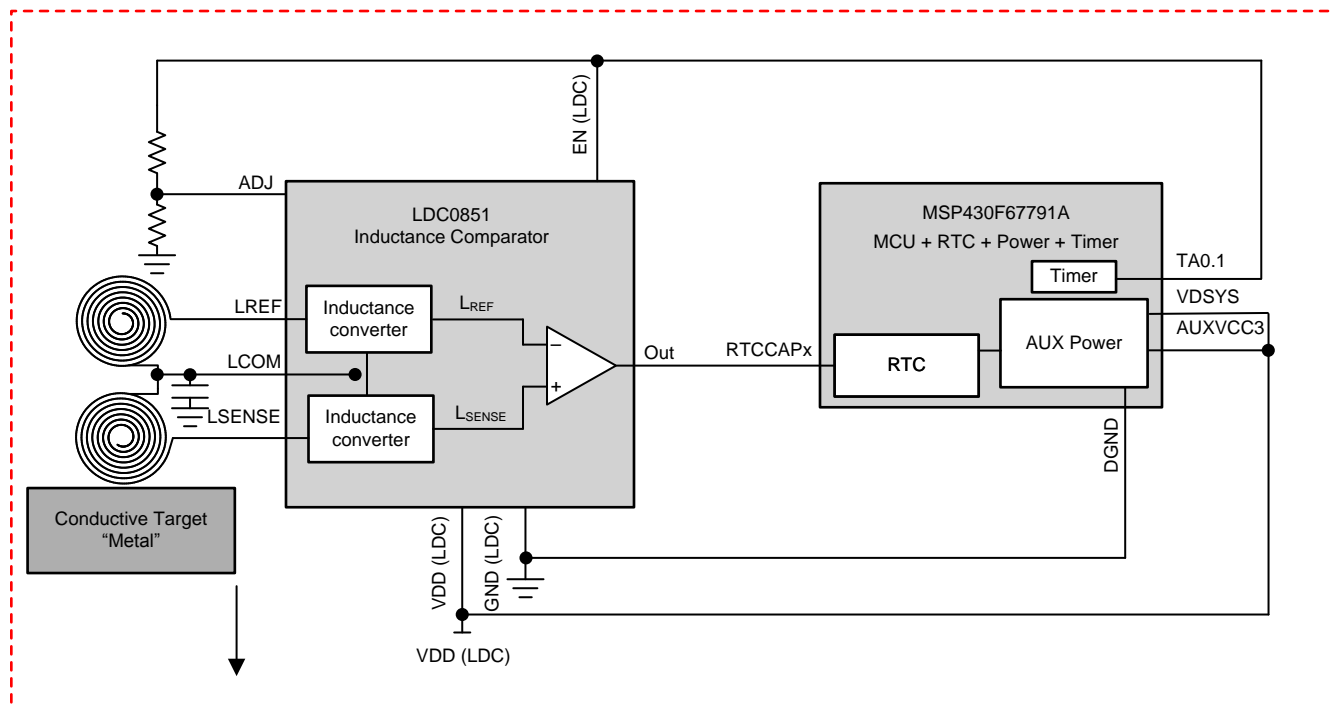


図 1. System Block Diagram—One-Sense-Coil Variant

For the one coil variant, only one sense coil is connected between the LSENSE and LCOM pins to sense the opening of the terminal block cover. For this variant, a conductive target metal is placed above the sense coil so that the sense coil has the smallest inductance when the terminal block cover is closed. This sense inductance value is sufficiently smaller than the adjusted reference coil inductance so that the LDC0851 output can be asserted low.

When the terminal block cover is opened, the distance between the target metal and sense coil increases, which causes the inductance value of the sense coil to increase. The inductance of the sense coil eventually increases until it is sufficiently larger than the adjusted reference coil so that the output can be asserted high, which indicates a case tampering event.

The second variant is a two-sense-coil implementation that detects when the terminal block cover and the main cover are opened. 図 2 shows the block diagram of the two sense variant of this design.

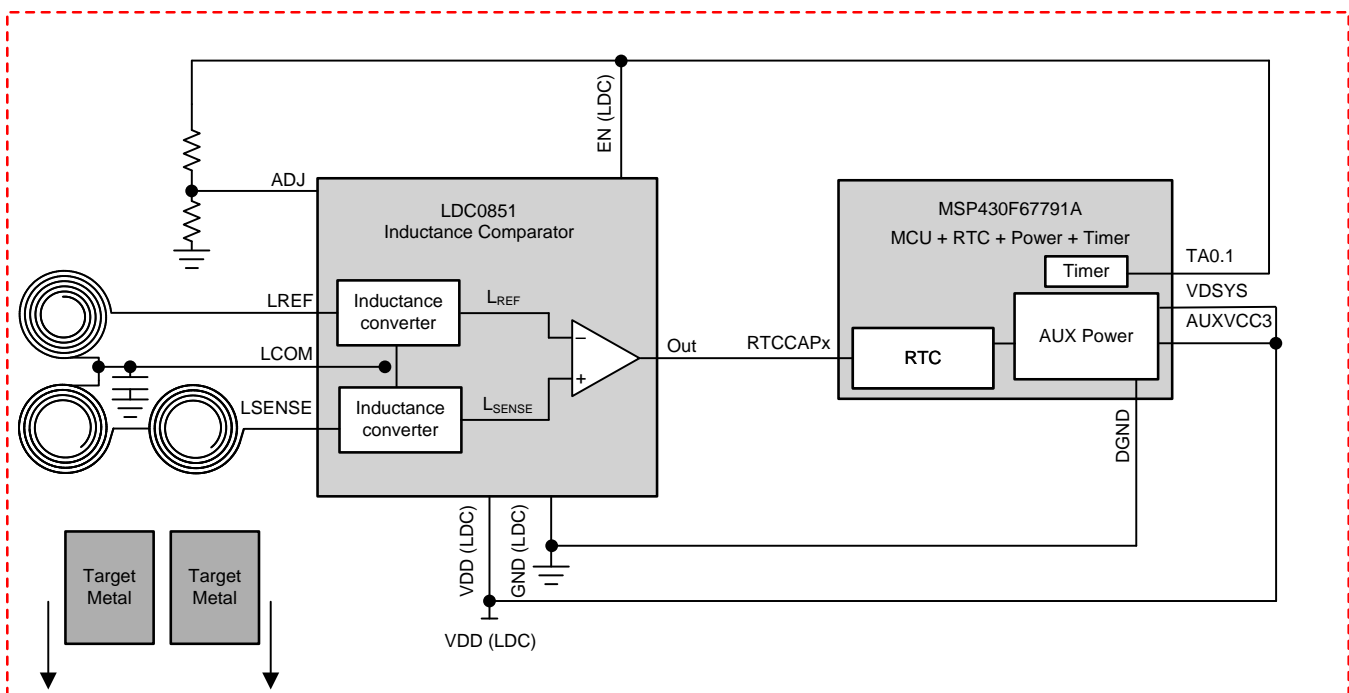

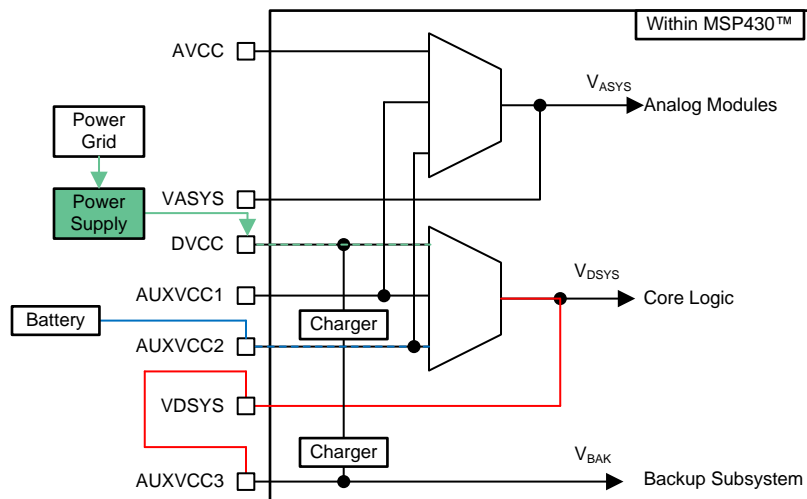


図 2. System Block Diagram—Two-Sense-Coil Variant

For this two-sense-coil variant, there is a series combination of two coils connected between the LSENSE and LCOM pins to detect the opening of both the terminal block cover and the main cover. For the two-sense-coil variant, both sense coils have their respective target metals placed above them so that each coils inductance, and therefore the equivalent inductance seen between LSENSE and LCOM pins, is the smallest when both the terminal block cover as well as the main cover are closed.

The two coil implementation works in a similar matter as the one coil implementation; however, to detect the opening of either the terminal block cover or the main cover, regardless of the state of the other cover, the inductance increase from opening the terminal block cover when the main cover is fully closed (and vice versa) must be large enough for the equivalent inductance of these coils to be sufficiently large with respect to the reference inductance. This parameter must be satisfied for the LDC0851 output to be asserted high to indicate tampering.

When the output of the LD0851 indicates the occurrence of case tampering, the MSP430F67791A logs the date and time of the first case tamper event and drives the light-emitting diodes (LEDs) and characters on a liquid-crystal display (LCD) to indicate if the case remains open. In addition to logging case tamper events, the MSP430F67791A also provides backup power to itself as well as the LDC0851 through the use of its AUX peripheral. This peripheral allows multiple power sources to power the MSP430™ MCU and LDC0851 switch.  3 shows the AUX module configuration for this design.



**図 3. AUX Module Configuration**

In the AUX module for the MSP430F67791A, the VASYS supply is used to power the analog parts of the chip while the VDSYS line is used to power the digital parts of the MSP430. The AUXVCC3 supply powers the RTC and tamper capture general-purpose input/output (GPIO) as well as the LDC0851. These supplies can be sourced from the DVCC and AVCC supplies or AUXVCC2. When selecting any of the power supplies for powering VASYS, the same supply is used for powering VDSYS. In a typical use case, AVCC and DVCC is connected to mains and AUXVCC2 is connected to a battery. In this design, whenever the power at DVCC is unavailable, the system is configured to automatically switch the selected power supply to AUXVCC2 if it is available. Both the MSP430™ MCU and LDC0851 switch can be powered by using this feature, even if there is a power outage.

When running off of a backup supply, reducing the current consumption of the system is important. In this design, the MSP430F67791A reduces the average current consumption of the LDC0851 device by driving the enable pin of the LDC0851 so that it can only be enabled for the amount of time necessary to obtain a valid reading. By only turning on the LDC0851 for the time necessary for a valid reading, the average current consumption of the LDC0851 is minimized to an approximate 2  $\mu$ A.

## 2.2 Highlighted Products

### 2.2.1 LDC0851

The LDC0851 is a close-range inductive switch which is ideal for contactless and robust applications such as presence detection, event counting, and simple buttons.

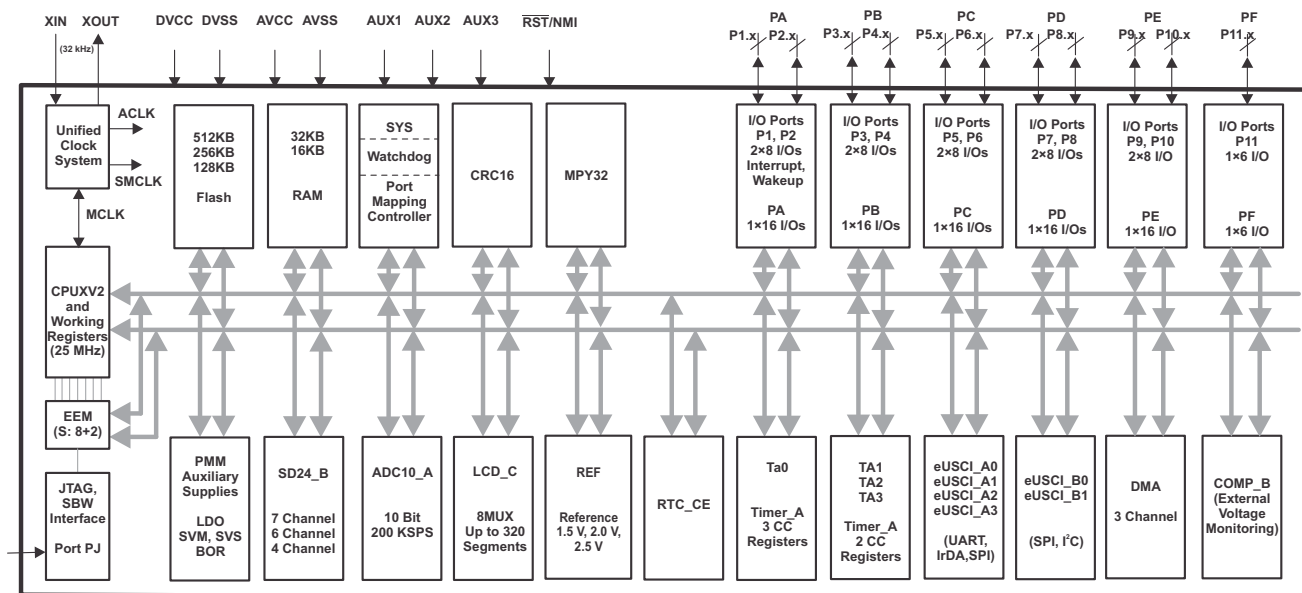
The switch is triggered when a conductive object comes within close proximity of the sensing coil. Hysteresis is included to ensure a reliable switching threshold immune to mechanical vibration. The differential implementation prevents false triggering over environmental factors such as temperature variation or humidity effects.

Inductive sensing technology provides reliable and accurate sensing even in the presence of dirt, oil, or moisture making the device ideal for use in harsh or dirty environments. The solid-state switching eliminates the failures due to reed, mechanical, or contact switching. Unlike competitive products, the LDC0851 does not require magnets, nor is it affected by DC magnetic fields. A summary of the device features is as follows:

- Threshold tolerance: < 1% of coil diameter
- Temperature stable-switching operation
- Average supply current: < 20  $\mu$ A at ten samples per second
- Shutdown supply current: 140 nA
- Push-pull output
- Resistor programmable threshold
- Insensitive to DC magnetic fields
- Contactless switching operation
- Supply voltage: 1.8 V to 3.3 V
- Operating temperature range:  $-40^{\circ}\text{C}$  to  $125^{\circ}\text{C}$

## 2.2.2 MSP430F67791A

Figure 4 shows a block diagram that displays the features of the MSP430F67791A.



Copyright © 2017, Texas Instruments Incorporated

Figure 4. MSP430F67791A Block Diagram

The MSP430F67791A belongs to the powerful 16-bit MSP430F6xx platform. This device finds its application in energy measurement and has the necessary architecture to support it. The MSP430F67791A has a powerful 25-MHz CPU with MSP430CPUx architecture. The analog front end (AFE) consists of seven independent 24-bit sigma-delta ( $\Sigma\Delta$ ) analog-to-digital converters (ADC) based on a second-order  $\Sigma\Delta$  architecture that supports differential inputs. The  $\Sigma\Delta$  ADCs ( $\Sigma\Delta 24\_B$ ) operate



independently and are capable of 24-bit results. The ADCs can be grouped together for simultaneous sampling of voltages and currents on the same trigger. In addition, the  $\Sigma\Delta$  module also has an integrated gain stage to support gains up to 128 for amplification of low-output current sensors. A 32-bit x 32-bit hardware multiplier on this chip can be used to further accelerate math-intensive operations during energy computation.

The RTC module on this device supports both offset and temperature compensation to ensure accurate time keeping. Additionally, the real-time clock (RTC) module supports automatic logging of an external event or tamper detection attempt. Other features of this chip include a module for switching between main and backup power sources.

### 3 System Design Theory

#### 3.1 Inductive Sensing Theory

The LDC0851 operates by generating an AC current through both the external reference and sense coils. When an AC current flows through an inductor, an AC magnetic field is produced. If a conductive material such as a metal object is brought near the coil, the magnetic field induces an eddy current on the surface of the target conductor, as 図 5 shows.

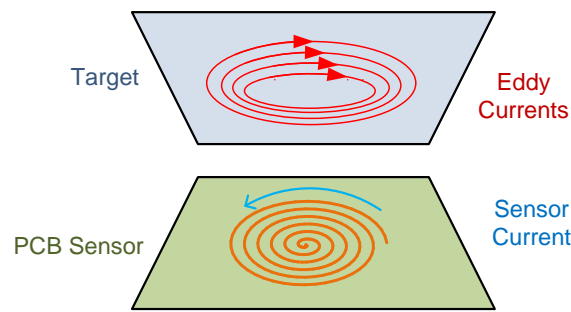


図 5. Eddy Current Generation

The eddy current generated is a function of the distance between the inductor and target metal, the size of the conductor, and the metal material. The induced eddy current generates its own magnetic field, which opposes the original magnetic field. As a result of the opposing magnetic field, the original magnetic field is weakened, which causes a decrease in inductance compared to its inductance when a conductive material is not present in proximity (also called the free-space inductance). For systems with multiple inductors in series, the decrease in inductance of one of the coils cause a decrease in the equivalent inductance of the combination of the coils.

An L-C resonator can be used, such as the series R-L-C construction shown in 図 6, to properly sense the change in inductance. For inductive sensing applications, the resistive element in this model represents parasitic circuit losses and is not a discrete component.

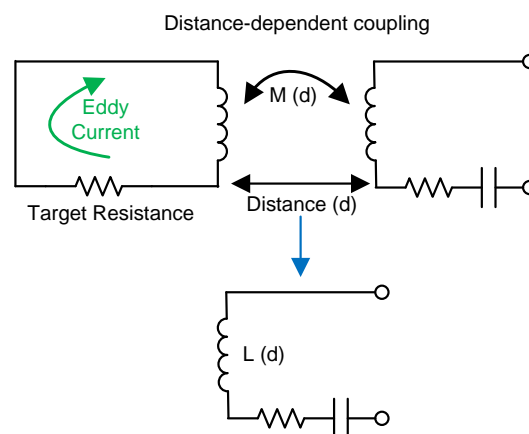


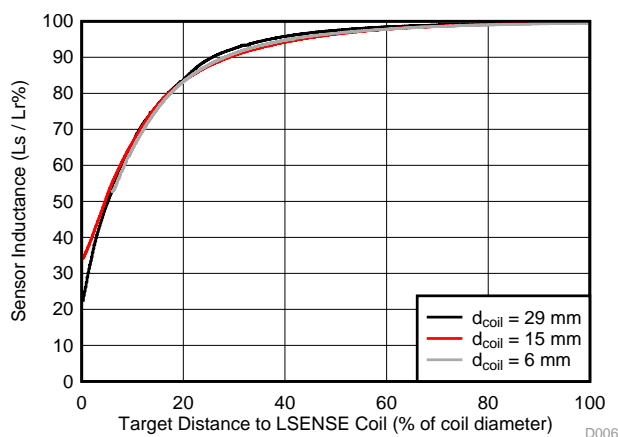
図 6. Electrical Model of Series Inductive Sensor

The resultant inductance in this model is dependent on the distance from the target metal to the inductor. The closer the target is placed, the smaller the resulting inductance. This decrease in the effective inductance of the L-C resonator can be observed as an increase in its resonating frequency given by 式 1. For multiple inductors in series, note that L in this equation represents the total equivalent inductance and not the inductance of an individual coil.

$$f = \frac{\sqrt{2}}{2\pi\sqrt{L \times C}} \quad (1)$$

The LDC0851 senses the inductance of an LC tank resonator that is implemented with PCB coils and an external capacitor. This device specifically compares the reference inductance with the sense inductance and changes its output based on which of the two has less inductance. For the one-sense-coil variant of this design, a metal that is connected to the meter case is placed above the sense coil so that the sense inductance is sufficiently less than the reference inductance when the terminal block cover is fully closed and the sense inductance is sufficiently greater than the adjusted reference inductance when the terminal block cover is opened. For the two-sense-coil implementation, a separate target metal is placed above each sense coil so that the equivalent sense inductance of the two sense coils is sufficiently less than the reference inductance when both the terminal block cover and main cover is closed while still being sufficiently greater than the adjusted reference inductance when either the terminal block or main cover is opened. As a result, the LDC0851 output is either asserted high or low based on whether the case is opened or closed.

図 7 shows an example of how the sense coil inductance changes for three different coil diameters as the target metal is placed near the sense coil of the LDC0851. In this graph, similar to the TIDA-01377 design, the distance from the target metal to the sense coil is varied while the reference coil does not have a metal near it so the reference inductance value is fixed. Also note that the sense and reference coils are physically similar in this graph, which means that they have approximately equal free-space inductances.



**図 7. Sensor Inductance versus Target Distance**  
**L<sub>SENSE</sub> Inductance (L<sub>s</sub>) Varied, L<sub>REF</sub> Inductance (L<sub>r</sub>) Fixed**

The resultant sense inductance shown in 図 7 is dependent on coil diameter, distance from the coil to the target metal, and free-space inductance value. As a result, normalizing the inductance results to show the inductances for different coil diameters is necessary. In this figure, this normalization is done on the y-axis by first representing the inductance value as a % ratio between the resultant sense coil inductance and the reference coil inductance, where the reference coil inductance must be approximately equal to the free space inductance of the sense coil. Moving down the y-axis corresponds to a larger decrease in inductance. For the x-axis, normalization is done by representing the distance from the coil to target metal

as a % ratio between the value of the distance between the coil and metal to the value of the coil diameter. In this figure, moving to the left on the x-axis represents placing the target metal closer to the sensor coil. An observer can conclude from this figure that the closer the target metal is placed near the sense coil, the smaller the value of the inductance. Based on 式 1, a smaller inductance value means a larger sensor frequency. As a result, placing a metal closer to the sense coil increases the sensor frequency, as 図 8 shows.

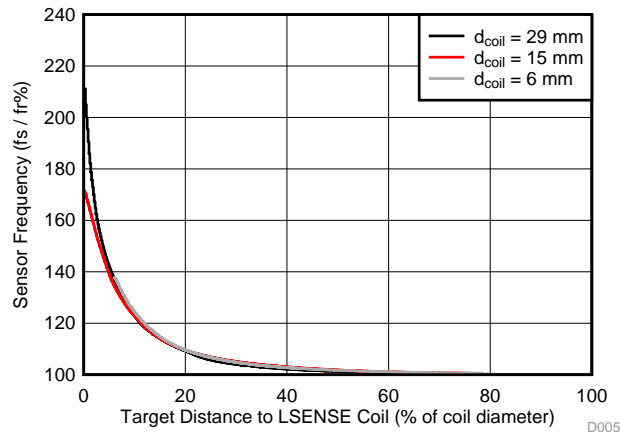


図 8. Sensor Frequency versus Target Distance  
L<sub>SENSE</sub> Frequency (f<sub>s</sub>) Varied, L<sub>REF</sub> Frequency (f<sub>r</sub>) Fixed

For more details on inductive sensing theory, see the [LDC0851 Quick-Start Guide](#) application note [2].

### 3.1.1 Effect of Magnetic Fields

The LDC0851 operates on the principle of inductive sensing using an LC resonator circuit, which inherently provides immunity to all frequencies that fall outside the passband of the LC tank, including DC magnetic fields. For more information, see the following blog post: [Inductive sensing: Are narrow-band LC sensors immune to DC magnetic fields?](#) [3]. Due to the high Q of the design, the LDC0851 can only be affected by fields that have a frequency that is precisely near the sensor frequency of the LDC0851, which is difficult to happen. Theoretically, even if it is possible to generate a strong magnetic field sufficiently close enough to the LDC0851 sensor frequency, the LDC0851 is not disabled. Instead, the magnetic field only causes the LDC0851 output to constantly switch between states, causing the MSP430 MCU to log this as a tamper attack.

## 3.2 LDC0851 Sensing Components

図 9 shows the LDC0851 sensing components. The LDC0851 sensing circuitry primarily consists of the LDC0851 inductive switch core that drives the total capacitance, sense inductor, and reference inductor, where the sense and reference inductors can each be implemented as one inductor or multiple inductors in series.

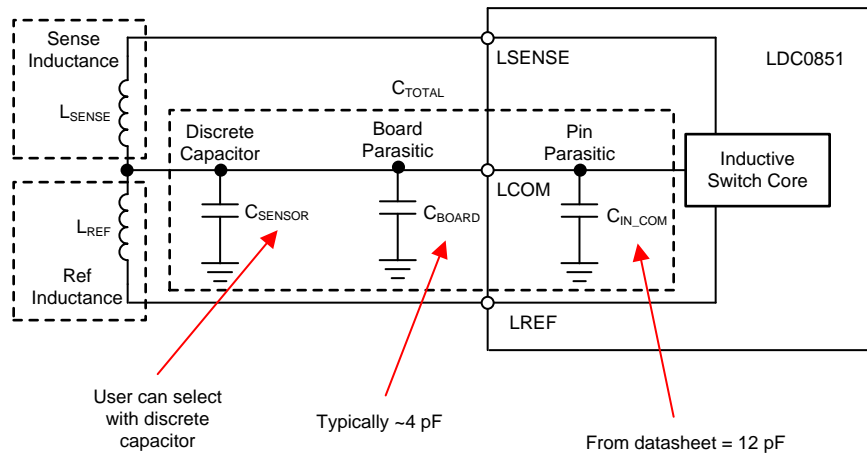


図 9. LDC0851 Sensing Components

As 式 2 shows, the total capacitance is the sum of the parasitic capacitance from the LCOM pin, the parasitic capacitance from the PCB, and the discrete capacitor. The *LDC0851 Differential Inductive Switch* data sheet shows the parasitic capacitance from the LCOM pin to be 12 pF. The board parasitic capacitance is typically 4 pF; however, a more accurate value of the board parasitic capacitance can be found by measuring the capacitance of the PCB when it has no components populated. The sensor capacitance is selected by the user as a way to adjust the total capacitance. One constraint for proper operation of the LDC0851 is that the total capacitance must be greater than 33 pF, as shown in 式 3.

$$C_{TOTAL} = C_{BOARD} + C_{IN\_COM} + C_{SENSOR} \quad (2)$$

$$C_{TOTAL} > 33 \text{ pF} \quad (3)$$

A similar constraint exists for the sensor inductance in that the equivalent sensor inductance must be greater than the minimum inductance value as defined by 式 4:

$$L_{SENSOR} \geq \frac{1}{4.83 \times f_{SENSOR} \times I_{SENSOR\_MAX}} \quad (4)$$

where,

- $I_{SENSOR\_MAX}$  can be found in the *LDC0851 data sheet*.

The total capacitance, along with this sense inductance, determines the frequency of the sensor. 式 5 shows how to calculate this sensor frequency, which must be less than 19 MHz for proper operation of the LDC0851. The 19-MHz frequency constraint in 式 6, as well as the  $L_{SENSOR}$  constraint in 式 4, must remain in consideration when the target metal is placed closest to the sense coil because this action results in both the smallest inductance as well as the largest sensor frequency.

$$f_{SENSOR} = \frac{\sqrt{2}}{2\pi\sqrt{L_{SENSE} \times C_{TOTAL}}} \quad (5)$$

$$f_{SENSOR} < 19 \text{ MHz} \quad (6)$$

### 3.2.1 Sensor Component Implementation

#### 3.2.1.1 One-Coil Set Implementation

For the variant of this design that only detects the opening of the terminal block, 表 2 shows the values of the sensor components and parameters derived from these components. The inductance and sensor frequency varies with the distance from the sensor coil to target metal; therefore, the inductance and sensor frequency values are calculated for two sensor-coil-to-target-metal distances.  $d_{\text{UPPER\_BOUND}}$  corresponds to an upper-bound distance when a metal is not placed near the sensor coil. The maximum sensor-coil-to-target-metal distance in this design is less than this  $d_{\text{UPPER\_BOUND}}$ .  $d_{\text{LOWER\_BOUND}}$  corresponds to a lower-bound distance when the metal is placed closer to the sensor coil than the minimum sensor-to-target-metal distance used in this design.

**表 2. Sensor Component Values and Constraints for One-Sense-Coil Implementation**

PARAMETER	VALUE
$C_{\text{SENSOR}}$	27 pF
$C_{\text{TOTAL}}$ constraint	$C_{\text{TOTAL}} > 33 \text{ pF}$
$C_{\text{TOTAL}}$	43 pF
$L_{\text{SENSOR}}(d_{\text{UPPER\_BOUND}})$ constraint	$L_{\text{SENSOR}}(x) > 2.203 \mu\text{H}$
$L_{\text{SENSOR}}(d_{\text{UPPER\_BOUND}})$	4.801 $\mu\text{H}$
$f_{\text{SENSOR}}(d_{\text{UPPER\_BOUND}})$	15.665 MHz
$L_{\text{SENSOR}}(d_{\text{LOWER\_BOUND}})$	4.247 $\mu\text{H}$
$f_{\text{SENSOR}}(d_{\text{LOWER\_BOUND}})$	$f_{\text{SENSOR}}(d_{\text{LOWER\_BOUND}}) < 19 \text{ MHz}$
$f_{\text{SENSOR}}(d_{\text{LOWER\_BOUND}})$	16.656 MHz

Based on 式 4, an assumed 3.3-V supply voltage (resulting in an  $I_{\text{SENSOR\_MAX}}$  value of 6 mA), and the sensor frequency, the minimum inductance constraint is calculated. This constraint is calculated for a target metal-to-coil distance of  $d_{\text{LOWER\_BOUND}}$  because it results in the largest value of minimum inductance. The range of sensor inductance values meet this minimum sensor inductance constraint. In addition to meeting the minimum inductance constraint, the sensor components also meet the minimum total capacitance constraint (式 3) and the maximum sensor frequency constraint (式 6). For the maximum sensor frequency constraint, it is only necessary to compare  $f_{\text{SENSOR}}(d_{\text{LOWER\_BOUND}})$  to the 19-MHz limit because the sensor frequency is the largest at the closest target-metal-to-sense-coil distance.

#### 3.2.1.2 Sensor Component Values and Constraints for Two-Sense-Coil Implementation

The two-sense-coil implementation implements the same sense coil used to sense the opening of the terminal block cover for the one-coil implementation with a few slight modifications. In addition to this terminal block coil, the two-sense coil implementation uses an additional coil to sense the opening of the main cover. For this additional coil, a copy of the terminal block coil was used and slightly modified. The terminal block coil and the main cover coil were placed in series and then connected to the LDC0851 device. This action resulted in a total sense inductance of 9.744  $\mu\text{H}$ . The reference coil is designed to match this inductance value. 表 3 shows the values of the sensor components and parameters derived from these components for the two-sense-coil variant, where these parameters are well within the LDC0851 constraints derived from these sensor components.

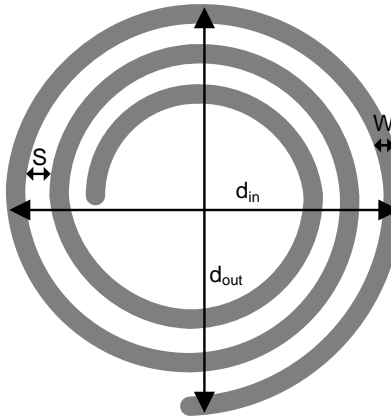
**表 3. Sensor Component Values and Constraints for Two-Sense-Coil Implementation**

PARAMETER	VALUE
$C_{\text{SENSOR}}$	27 pF
$C_{\text{TOTAL}}$	43 pF
$L_{\text{SENSOR}}(d_{\text{UPPER\_BOUND}})$	9.774 $\mu\text{H}$
$f_{\text{SENSOR}}(d_{\text{UPPER\_BOUND}})$	10.996 MHz

### 3.3 Coil Design

#### 3.3.1 Coil Construction and Constraints

One possibility for the sense and reference inductor implementation is to fabricate coils onto the system PCB itself. 図 10 shows an example of the geometry of a PCB coil.



**図 10. Example PCB Coil Geometry**

In 図 10,  $d_{\text{in}}$  represents the inner diameter of the coil,  $d_{\text{out}}$  represents the outer diameter of the coil,  $w$  represents the trace width of the coil, and  $s$  represents the spacing between the traces used in the coils. The outer diameter of the coil is one of the factors that determines the distances at which the LDC0851 device switches states (the larger the outer coil diameter, the larger the switching distance). When designing the coils for the LDC0851 device, TI recommends that the ratio of  $d_{\text{in}}$  to  $d_{\text{out}}$  be within the limits shown in 式 7.

$$0.2 < \frac{d_{\text{in}}}{d_{\text{out}}} < 0.8 \quad (7)$$

Verify that the area for coil placement has enough room before designing the coils (see 式 8).

$$d_{\text{out}} < d_{\text{max}} \quad (8)$$

To increase the inductance of the sense and reference inductor, coils can be placed on multiple layers of the PCB and then connected to each other using a via. 図 11, 図 12, and 図 13 show a two-layer coil implementation. The final inductance value depends on factors such as  $d_{\text{in}}$  (this can be approximated from  $d_{\text{out}}$ ,  $s$ ,  $w$ , and the number of turns of the coil),  $d_{\text{out}}$ , the number of turns of the coil, the number of coil layers, as well as the distance between the coil layers.

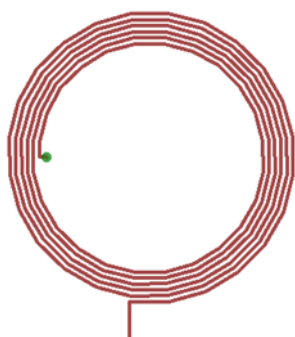


図 11. Top Layer Coil

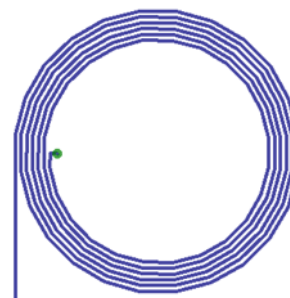


図 12. Bottom Layer Coil

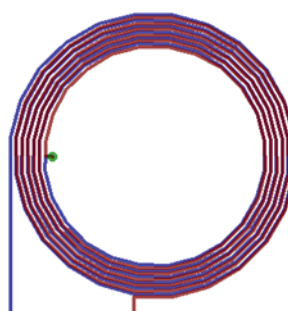


図 13. All Coil Layers



### 3.3.2 Coil Solution Type and Switching Distance

To prevent the false switching of the LDC0851 output, internal hysteresis is included for the switching threshold as shown in 図 14. The switch ON (LDC0851 output asserted LOW) and switch OFF (LDC0851 output asserted HIGH) points are both determined by the ratio of the equivalent sense inductance to the equivalent adjusted reference inductance, which can be correlated to distance for proximity applications.

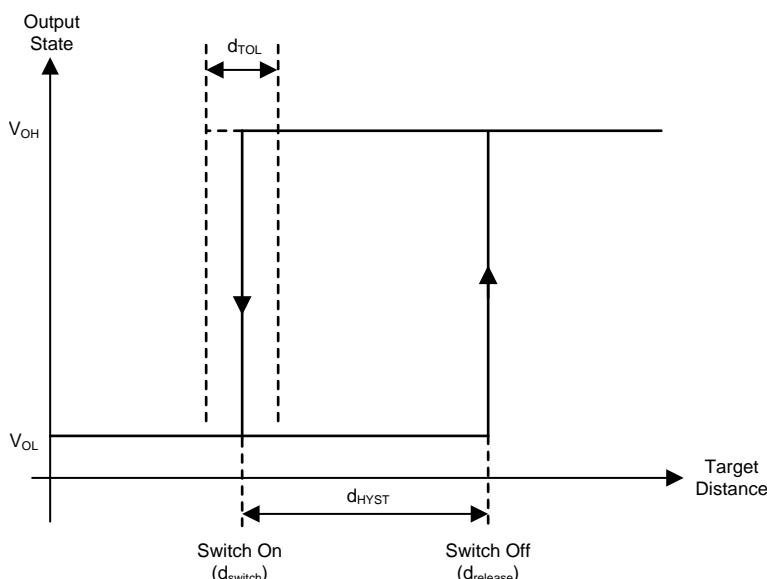


図 14. Switching Distance Hysteresis and Threshold Tolerance

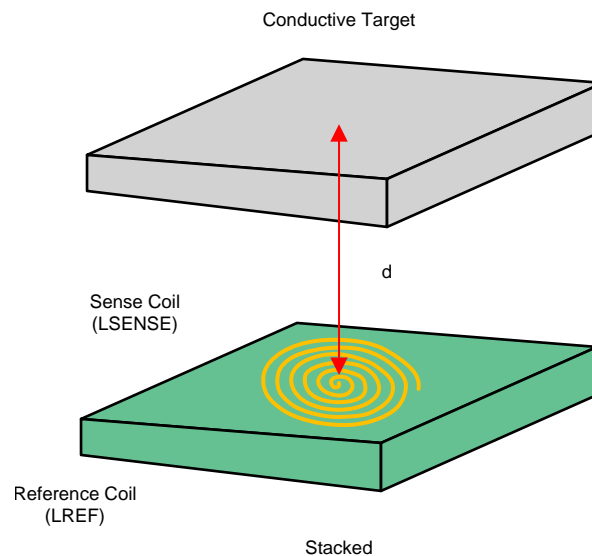
For the one-sense-coil variant of this design, when the terminal block cover is fully closed, the target metal-to-sense-coil distance is the smallest. For this scenario, the distance from the target metal to sense coil is smaller than the switch ON distance, so the LDC0851 output is asserted low. As the case is being opened, the distance from the target metal to sense coil increases. When this target metal-to-sense-coil distance increases to greater than the switch OFF distance, the output of the LDC0851 is asserted high, which indicates a case tamper event. To properly detect case tampering, the switch ON and switch OFF distances must be within the range of motion of the target distance. For the switch ON distance, this means that the minimum distance from the target metal to the sense coil ( $d_{target,min}$ ) must be less than the switch ON distance, as is shown in 式 9. For the switch OFF distance, the maximum distance from the target metal to the sense coil ( $d_{target,max}$ ) must be greater than the switch OFF distance, which is also shown in 式 9. Note that the switch ON and switch OFF distances cannot both be set independently. Designing the switch ON distance also sets the switch OFF distance.

$$d_{target,min} < d_{switch} < d_{release} < d_{target,max} \quad (9)$$

When using multiple sense coils in series, the switching points are still determined by the same inductance ratio as discussed previously; however, the correlation to distance now changes because each series coil contributes a small portion to the overall inductance shift. As a result, to ensure the proper switching of the LDC0851 output for the two-sense-coil variant of the design, the total minimum sense inductance when each target metal is the closest to its corresponding sensor coil is designed to be sufficiently lower than the total adjusted reference inductance so that the LDC0851 output can be asserted low in the nominal, unopened state. Additionally, to sense openings at multiple locations regardless of the open or closed state at the other locations, the inductance of each sense coil when its corresponding target metal is the furthest from it is designed so that this inductance is sufficiently large. This specific inductance for each coil must be large enough for the total equivalent sense inductance to be sufficiently

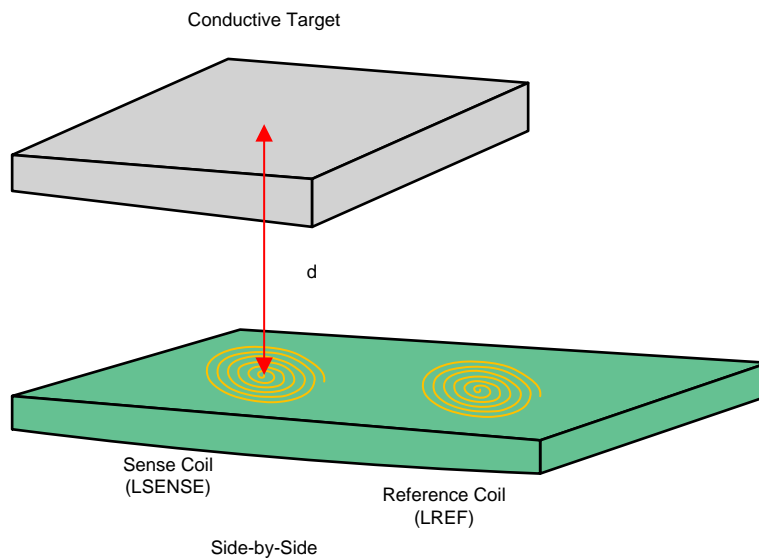
larger than the total adjusted reference inductance so that the LDC0851 output can be asserted high, even if all the other coils are at their minimum inductance values due to having their target metals closest to them. By doing this, the total inductance when the terminal block cover was opened but the main cover was completely closed was still large enough for the LDC0851 output to be driven high. Similarly, the total inductance when the main cover was opened but the terminal block cover was completely closed was also still large enough for the LDC0851 output to also be driven high.

One of the factors that determines the switching distance for a one-sense-coil implementation is whether a stacked or side-by-side coil solution is used. [Figure 15](#) shows a stacked coil solution. This solution is used when the designer wishes to conserve board space. A four-layer PCB with a thick inner layer is recommended for the best results. See more details on this coil solution type in the [LDC0851 data sheet](#).



**図 15. Stacked Coil Solution Type**

The side-by-side solution is recommended for systems that use a two-layer PCB or a four-layer PCB with a large available area for side-by-side coils. This side-by-side solution provides the best performance. In the solution that [Figure 16](#) shows, the reference and sense coils are placed next to each other on the same PCB instead of on top of each other. For this design specifically, a side-by-side coil is used with a two-layer PCB.



**図 16. Side-by-Side Coil Solution Type**

For a one-coil implementation, an approximation of the resulting switch ON distance for a side-by-side solution can be found by 式 10. For a multiple sense coil implementation, the switch ON distance associated with a particular coil depends on the parameters shown in 式 10 as well as the inductance values of the other coils in series with it because the equivalent inductance is what sets the switching distance.

$$d_{\text{SWITCH,SidebySide}} \approx d_{\text{out}} \times 0.4 \times \left( 1 - \frac{\text{ADJ}_{\text{CODE}}}{16} \right) \quad (10)$$

As 式 10 shows, one of the factors that determines the switching distance is a constant that is called the  $\text{ADJ}_{\text{CODE}}$ . The  $\text{ADJ}_{\text{CODE}}$  is used specifically to reduce the effort required to design the sense and reference coils precisely for a specific switching distance. This  $\text{ADJ}_{\text{CODE}}$  has 16 possible values where the selected code is chosen by applying a specific voltage on the ADJ pin of the LDC0851 by using a resistor divider network. This  $\text{ADJ}_{\text{CODE}}$  determines the amount of inductance to subtract from the reference inductance measurement to produce a new effective reference inductance value. By reducing the effective reference inductance value, the switch ON and switch OFF distances decrease. 図 17 shows how the switch ON and switch OFF distance changes based on a given ADJ code for a one-sense-coil implementation. The switching distance y-axis is normalized based on the coil diameter in this graph because the results for three different coil diameters have been used.

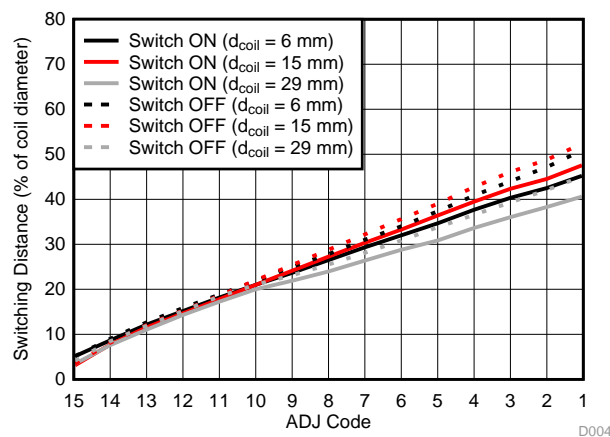


図 17. Switching Distance versus  $\text{ADJ}_{\text{CODE}}$

Note that the  $\text{ADJ}_{\text{CODE}}$  is used to reduce the switching distance and not increase the switching distance. The maximum switching distance is determined almost entirely by the coil diameter (which corresponds to  $\text{ADJ}_{\text{CODE}} = 0$ ). As a result, the best method is to design a coil with a larger coil diameter, which results in a larger switching distance than required. After designing the system, the ADJ code could then be modified on prototype boards to find the best ADJ value.

Based on the trends mentioned in 式 10, the system can be tweaked to meet any custom system constraints. For example, if the designer desires to have a specific switching, the diameter of the coil and  $\text{ADJ}_{\text{CODE}}$  can be modified to realize this switching distance. Alternatively, if there is no room to add a specific sized coil, a smaller diameter coil can be found by decreasing the  $\text{ADJ}_{\text{CODE}}$ , placing the target metal closer to the sense coils to reduce the desired switch ON and OFF distances, or both. 式 10 also shows that the minimum coil diameter supported is two and a half times the switching distance.

### 3.3.3 Using WEBENCH to Create Initial PCB Coils

A [LDC0851 WEBENCH](#) tool is available to facilitate PCB coil design for the reference and sense coils. This tool creates a preliminary reference and sense coil design based on certain parameters of the system. After creating a coil design, the design can be exported into the computer-aided design (CAD) tool used for the design of the system so that the coils can be integrated into the system PCB.

To use the WEBENCH tool, first go to the [LDC0851 WEBENCH](#) website. After visiting the page, a screen similar to [Figure 18](#) appears.

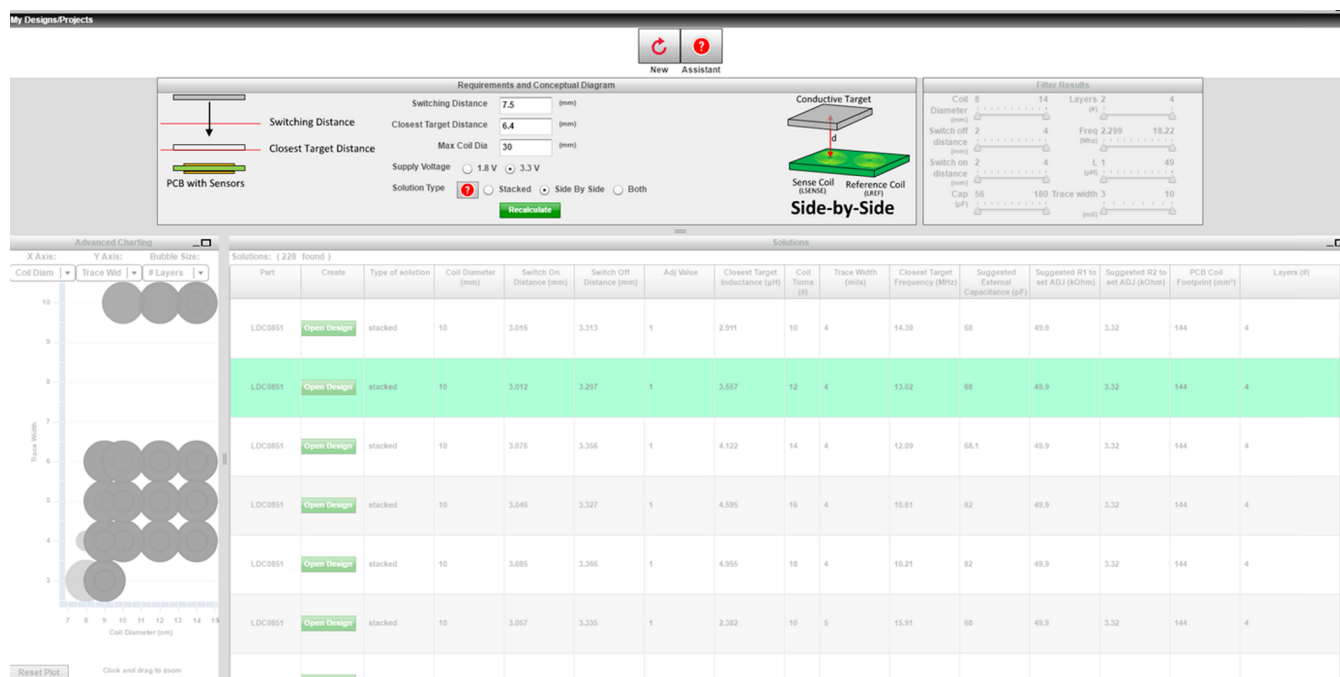


Figure 18. Initial LDC0851 WEBENCH Website

From this website, enter the switching distance ( $d_{\text{switch}}$ ), closest target distance ( $d_{\text{target,min}}$ ), max coil diameter ( $d_{\text{max}}$ ), supply voltage, and solution type (either stacked or side-by-side) in the *Requirements and Conceptual Diagram* section in the upper-left portion of the website. After entering these parameters, press the *Recalculate* button to generate an initial set of coils in the bottom-right portion of the website.

After an initial set of coils have been generated, the coils should be filtered based on the PCB constraints. Particularly, the number of layers of the PCB (to where the coils will be imported) must be filtered by constraining the *Layer (#)* filter to correspond to the number of PCB layers. In addition, the *Trace Width (mils)* filter should be adjusted to consider the minimum trace width supported by the PCB manufacturer for the design. The *Layer (#)* and *Trace Width (mils)* parameters are some of the parameters that determine the inductance of the coil. To reduce the average current consumption of the LDC0851, the *Freq* sensor frequency field can also be filtered to include coils that would result in higher sensor frequencies ( $> 10$  MHz). By applying the filters to the coil results, a screen similar to [Figure 19](#) appears.

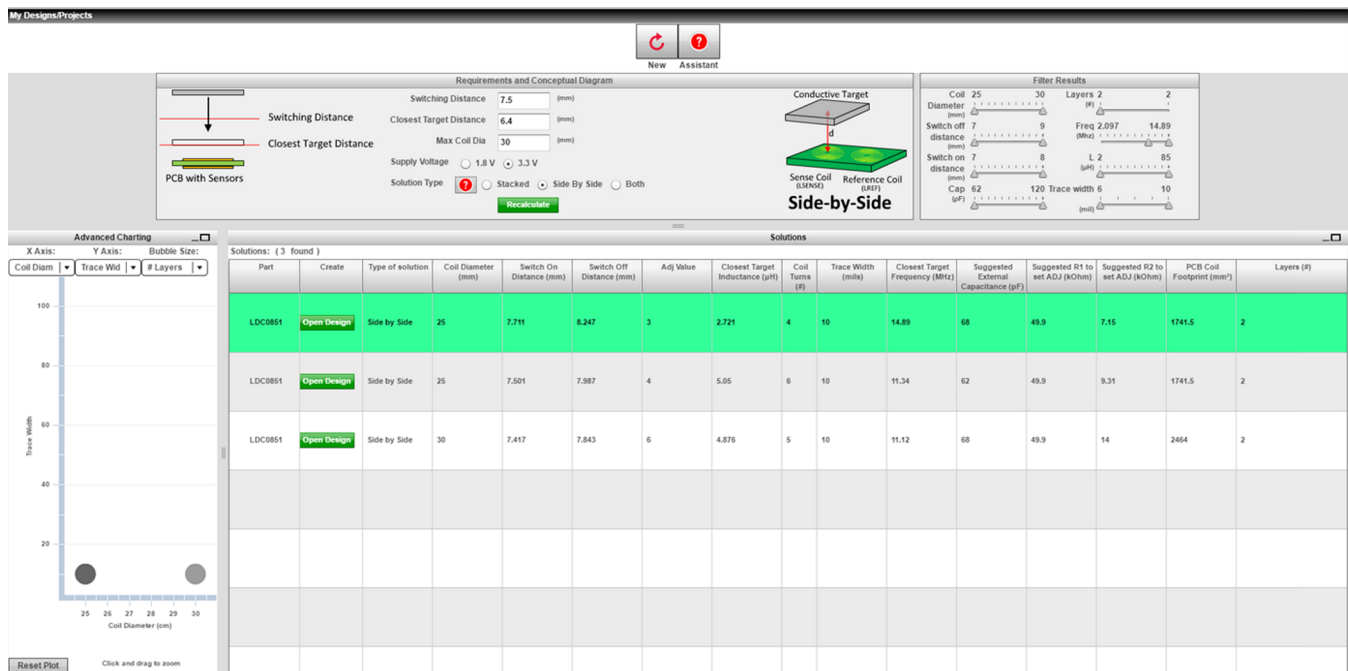


図 19. WEBENCH Results After Applying Filters

From the coils that resulted from applying the filters, the basic information on each coil can be obtained by clicking on the *Open Design* button shown in 図 19 for each coil. After pressing this button, a screen similar to 図 20 appears.

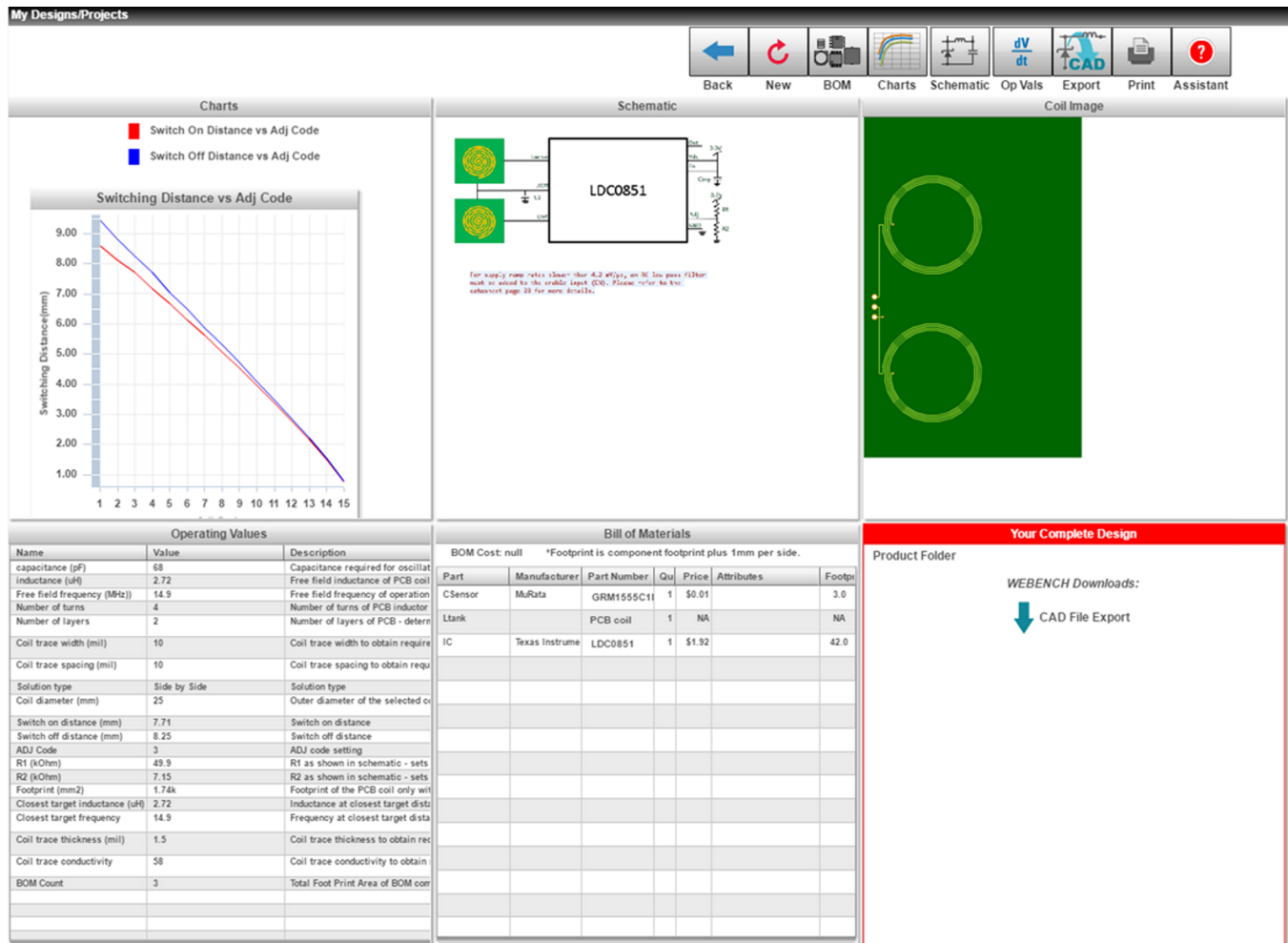


図 20. WEBENCH Coil Info Page

Press the *Op Vals* button near the top right of the WEBENCH Coil Info Page to obtain a full list of the coil parameters, as 図 21 shows.

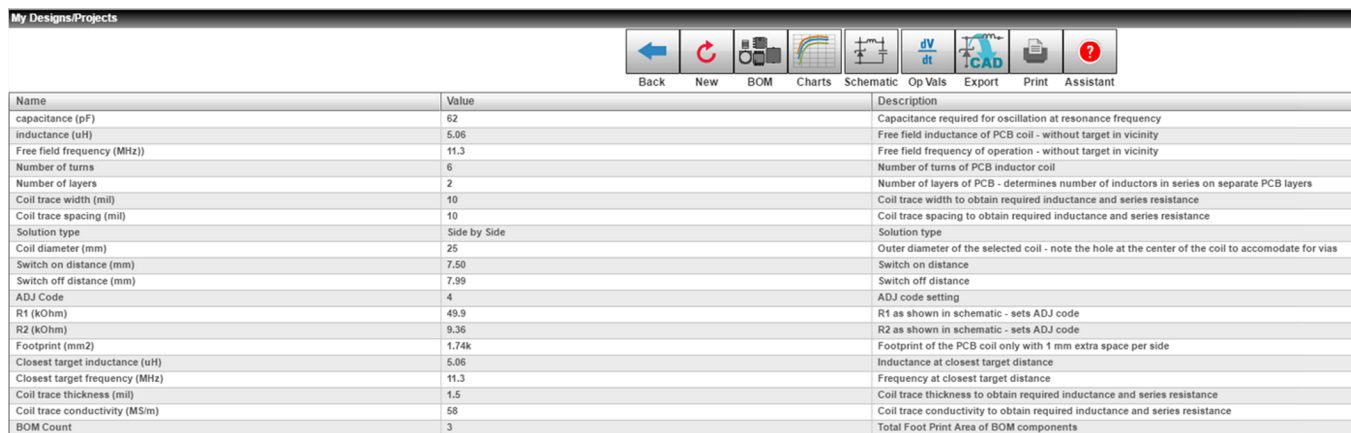


図 21. Coil Parameter Screen

For a one-sense-coil design, the designer should verify that the listed parameters on the coil parameter screen meet the coil and sensing constraints previously mentioned. If a design meets these constraints, then the coil can be exported to a selected CAD tool by pressing the *Export* button. For multiple sense coil systems, note that some of the parameters featured in this [Figure 21](#) are incorrect because the calculations are based using the inductance of a one sense coil instead of the total equivalent sense inductance.

### 3.3.4 Coil Implementation

#### 3.3.4.1 One-Sense-Coil Implementation

##### 3.3.4.1.1 Meter Case Mechanics and Sensing Locations for One-Sense-Coil Implementation

For the one-coil implementation, the opening of the terminal block cover is specifically detected as the case tamper event. In this design, the case tamper detection mechanism is designed based on the utilized, three-phase e-meter cover for the design. This case has two cover parts: One cover is the main cover in [Figure 22](#) and the other cover was the terminal block cover that goes on top of the main cover. On the main cover, there is an elevated area (see [Figure 23](#)) that causes a platform inside the main cover ([Figure 22](#)) to descend downward when the elevated area has been pressed. When the terminal block cover is placed on the main cover and screwed down as shown in [Figure 24](#), the platform is forced to descend downward.



Figure 22. Inside of Main Cover



Figure 23. Main Cover Placed on e-Meter Case





図 24. Terminal Block Cover Fully Screwed onto Main Cover

Two options exist for implementing detection of the terminal block cover opening. One option is to use the platform on the main cover shown in 図 22, which descends as the terminal block cover is screwed down. The second option is to have a PCB directly underneath the terminal block cover. Because the main cover is directly above the main PCB of the entire system, to place a PCB directly underneath the terminal block cover for the selected case a separate PCB would have to be placed directly on the terminal block. The first option is more feasible for the utilized meter case, so it is the implemented option for detecting the opening of the terminal block cover.

To detect case tampering using the platform of the main cover, the target metal is placed on the platform (see 図 25) so that the target metal moves up and down with the platform. The sensor coil of the LDC0851 is fabricated on the PCB directly underneath the target metal that is on the platform. The LDC0851 switches states based on the ratio of the sense inductance with respect to the reference inductance, which depends on the position of the metal on the platform with respect to the sensor coil. In the default state, when the terminal block cover is fully screwed down, the metal is at its closest distance ( $d_{\text{target,min}}$ ) with respect to the sense coil. This distance is less than the designed switching distance ( $d_{\text{switch}}$ ), so the LDC0851 output would be asserted low. As the terminal block is being removed, the platform with the metal ascends causing the distance between the metal and sensor coil to increase. When this distance is greater than the release distance ( $d_{\text{release}}$ ), the output of the LDC0851 changes to being asserted high and the MSP430 MCU logs this as a case tamper event.



**図 25. Case Platform With Metal Placed on Top**

For the terminal block tamper detection of this case, the closest target metal-to-sensor-coil distance ( $d_{\text{target,min}}$ ) is approximately 7 mm. The furthest target metal-to-sensor-coil distance ( $d_{\text{target,max}}$ ) is approximately 10 mm, which occurs when the terminal block cover is completely removed. To detect case tampering, the distances at which the LDC0851 switches ON ( $d_{\text{switch}}$ ) and switches OFF ( $d_{\text{release}}$ ) must be between 7 mm to 10 mm.

### 3.3.4.1.2 Optimizing One-Sense-Coil Layout

In this design, WEBENCH has been used to export initial coils which were slightly modified later for optimization. 図 26 shows the initial version of the coils that were exported from WEBENCH, where the top coil is the reference coil and the bottom coil is the sense coil. The first change made to the exported coils was a removed capacitor that was exported from WEBENCH. This capacitor, which was the sensor capacitor exported from WEBENCH, was removed because there was already a sensor capacitor in the design. In the design, TI recommends to place the sensor capacitor near the LDC0851 IC and use a C0G/NP0 capacitor.

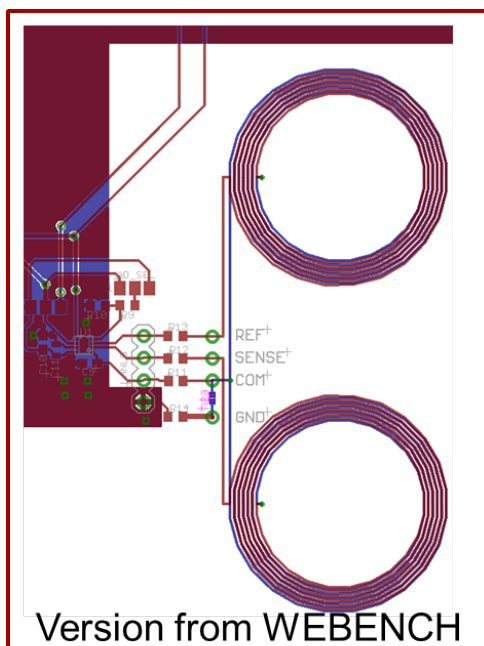


図 26. Initial Coils Exported From WEBENCH

When importing the coil, TI recommends that the distance from the coils to the ground plane should be at least half of the diameter of the PCB coils to prevent any interference. 図 27 shows how this change is made with respect to the layout shown in 図 26.

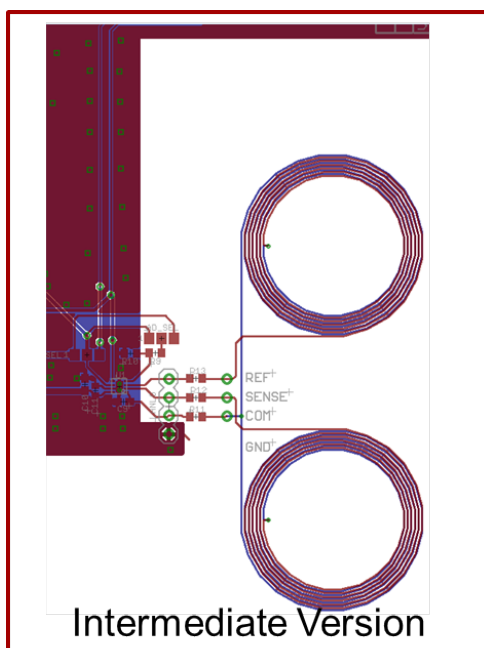


図 27. First Modifications Made to WEBENCH Coil

When designing a one-sense coil implementation, one of the most important layout guidelines to consider is that the reference and sense coil should be as symmetric as possible. Any asymmetry between these coils can cause an offset in inductance between the reference and sense coil inductances, which may affect the switching and release distances from their ideal values. In addition, having the sense and reference coil inductances equal leads to the best environmental tracking so that the system is least affected by environmental effects such as temperature variations.

To obtain better matching between the reference and sense coils, the coils were moved as shown in 図 27 so that the distance between each coil and the corresponding LDC0851 pin is closer than the coils initially exported from WEBENCH. After making the changes in 図 27, the number of crossings between the SENSE trace on the top layer (shown in red) with the bottom-layer COM trace (shown in blue) was changed from two to one so that the number of crossings matched the one crossing between the REF trace on the top layer and the COM trace on the bottom layer. In addition, the REF and SENSE traces on the top layer of the board were modified so that the crossing of these traces with respect to the COM trace is at a 90° angle to minimize the surface area and parasitic capacitance to improve matching. 図 28 shows the final version of the coils which is fabricated on the design.

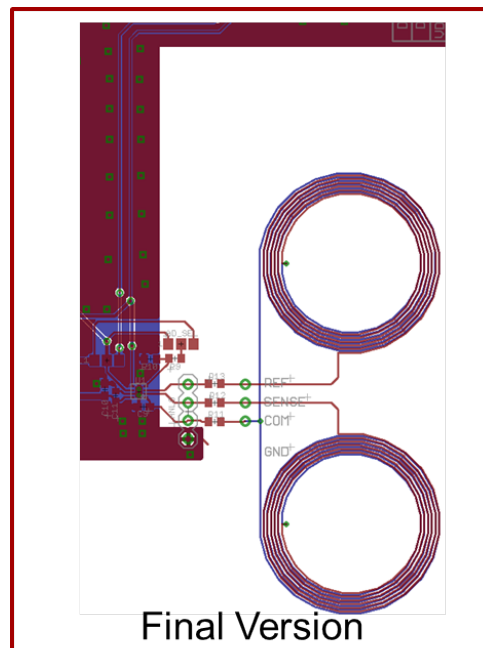


図 28. Coil Implemented in Design

In addition to the previously-mentioned guidelines, the designer should follow other basic layout guidelines such as monitoring the return current path.

#### 3.3.4.1.3 Implemented One-Sense-Coil Specifications

After plugging in the system parameters in the WEBENCH LDC0851 coil designer, a list of potential coils is generated. From the list of initial coils, the coils are further filtered so that the  $d_{\text{switch}}$  and  $d_{\text{release}}$  are within the range of movement of the target metal, as stated in 式 9. Given that the  $d_{\text{target,min}}$  distance corresponds to when the case is fully closed and the  $d_{\text{release}}$  distance is the minimum coil-to-target-metal distance for tampering to be detected, the terminal block cover would have to move a distance of

$d_{\text{release}} - d_{\text{target,min}}$  ( $\approx 0.99$  mm) for tampering to be detected for the one-sense-coil variant of this design. In addition, the ratio of  $d_{\text{in}} / d_{\text{out}}$  was checked to verify that it was within 0.2 to 0.8 as was recommended by 式 7. 表 4 shows the specifications of the final sense coil used in this design. The reference coil for the one-sense-coil implementation was designed to have an inductance approximately equal to the 4.801- $\mu\text{H}$  free-space inductance of the sensor coil.

**表 4. Implemented One-Sense-Coil Specifications**

PARAMETER	VALUE
Inner diameter( $d_{\text{in}}$ )	18.9 mm
Outer diameter( $d_{\text{out}}$ )	25 mm
$d_{\text{in}} / d_{\text{out}}$ constraint	$0.2 < d_{\text{in}} / d_{\text{out}} < 0.8$
$d_{\text{in}} / d_{\text{out}}$	0.76
Trace width (w)	10 mil
Spacing between traces (s)	10 mil
Number of turns on coil	Six turns
Number of PCB layers	Two layers
Free space inductance ( $L_{\text{SENSOR}}(d_{\text{UPPER\_BOUND}})$ )	4.801 $\mu\text{H}$
Turn ON distance ( $d_{\text{switch}}$ )	$\approx 7.5$ mm
Turn OFF distance ( $d_{\text{release}}$ , tampering)	$\approx 7.99$ mm
Change in terminal block cover position to trigger tampering	$\approx 0.99$ mm
ADJ <sub>CODE</sub>	4

### 3.3.4.2 Two-Sense-Coil Implementation

#### 3.3.4.2.1 Meter Case Mechanics and Sensing Locations for Two-Sense-Coil Implementation

For the two-coil implementation, the opening of the terminal block cover as well as the main cover is specifically detected as the case tamper event. In this design, the same terminal block detection mechanism used for the one coil variant is also used for the terminal block cover detection mechanism in this two-sense-coil implementation.

To sense the opening of the main cover, an additional sense coil is added. The sense coil is situated underneath the target metal; therefore, the locations where a target metal can be placed on the case determines the possible locations of the sense coil for the main cover. This target metal location must have some mechanism that allows the desired sensor coil to target metal distance. For this case specifically, the necessary target metal-to-sense-coil distance can be obtained by screwing in 7/8-inch standoffs in the holes shown in 図 29 and 図 30. After screwing in the two standoffs to the case, the target metal is placed on top of the two standoffs. Holes are then placed on the target metal to align with the screw holes on the top of the standoff. Next, screws are placed on top of the target metal and screwed into the standoffs so that the target metal is secured between the standoffs and the top of the screws. Another piece of copper tape is then placed on the side of part of the screwed-in target metal so that the target metal extends to the top-left inner side of the case, as 図 31 shows.

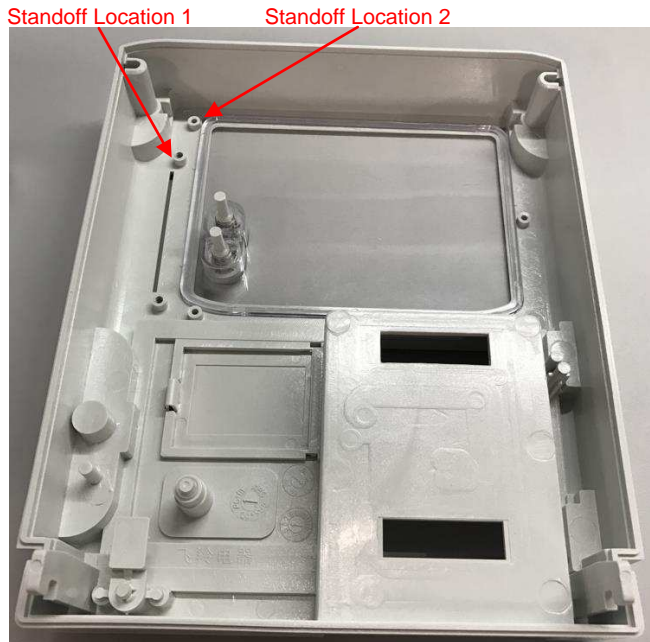


図 29. Standoff Locations

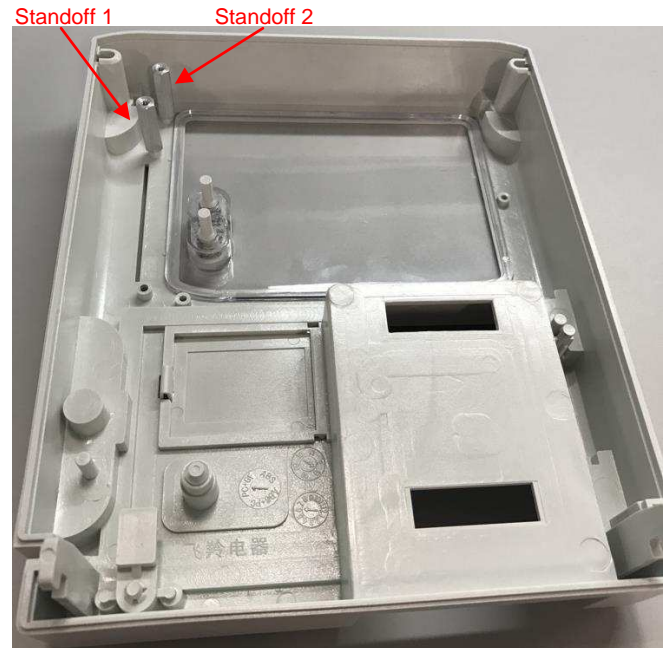


図 30. Standoffs Populated

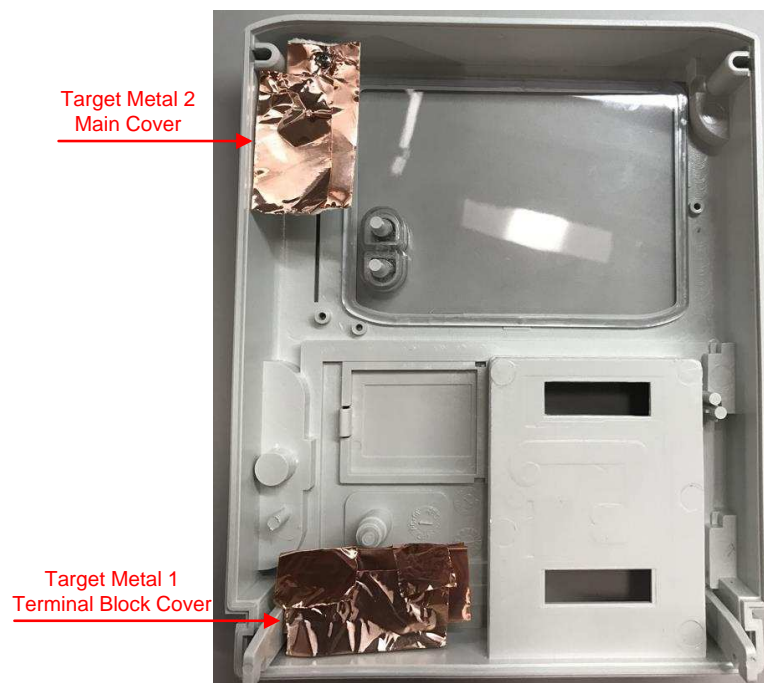


図 31. Target Metal Placement on Case

In the default state, when both the terminal block cover and the main cover are completely closed, the target metals distance to their corresponding sense coils is the smallest. Based on the mechanics of the main-cover target-metal placement, if the main cover is opened, the target metal of the main cover rises upward with the case, thereby causing the corresponding target metal-to-sense-coil distance to increase. This increase in target metal-to-sense-coil distance causes the inductance of the coil and, in turn, the total equivalent sense inductance to increase. When the total equivalent sense inductance is sufficiently larger than the reference inductance, the output of the LDC0851 switches high to indicate tampering.



### 3.3.4.2.2 Optimizing Two-Sense-Coil Layout

To sense openings at two locations, two sense coils must be placed in series with the series combination of these coils being connected to the LDC0851. The sense coil design must be set up so that any opening at one of the sense locations causes an increase in inductance for the corresponding coil, which in turn causes an increase in the total sense inductance that would be large enough to cause the LDC0851 output to switch to a high output state. In this design, similar coils were used for both sense coils; however, different coil diameters can be used for the different coils for other designs. When designing the different sense coils, a good starting point for the relative coil diameters based on the different desired switching distances can be found by using WEBENCH to design each coil to have the same ADJ value as if they were to be used in a single-sense coil implementation. Be sure to note that the final ADJ code for this series combination may drastically differ than this selected ADJ value for the single-sense coil scenario. The WEBENCH tool exports a one sense coil and one reference coil solution, so changes must be made to use multiple sense coils. Specifically, the sense portion of each coil design should be cut from their respective exported designs, pasted on the PCB of the final design, and then connected in series between the LCOM and LSENSE pins of the LDC0851 device.

After placing the sense coils, the reference inductance should ideally be designed to match the total sense inductance, which includes the sum of the individual sense coil inductance as well as the inductance of the traces used to connect the coils. Two options exist for the reference coil implementation. The first option is to have one reference coil that matches each sense coil and to have these reference coils in series the same way the sense coils are placed in series. This option allows for easy matching of the reference and sense inductances at the cost of board space and increased routing difficulty. The second option is to just have one reference coil and to try to match the inductance of this reference coil to the total sense inductance. This second option, which is implemented in the two coil variant of this design, is the most space efficient and simplifies the routing between coils. In this design, the reference coil was selected in WEBENCH by filtering different coil options to have an inductance close to the total sense inductance. After selecting the reference coil, the previous reference coil for the one-sense-coil implementation was replaced with this new coil and slightly modified for the final coil implementation.

Figure 32 and Figure 33 show the two-sense-coil implementation used in this design. In these figures, a trace on the top layer of the board connects the LDC0851 LSENSE pin and the top layer of sense coil 2, where sensor coil 2 is used to sense the opening at the main cover. A trace from the bottom layer of sense coil 2 is then connected to the top layer of sense coil 1, where sense coil 1 is used for sensing the opening at the terminal block cover. A trace from the bottom layer of sense coil 1 connects to the LCOM pin of the LDC0851. In comparison to these sense coils, the reference coil has a trace connected to its top layer, which is connected to the LREF pin of the LDC0851. The reference coil also has another trace connected on its bottom layer, which is connected to the LCOM pin of the LDC0851.

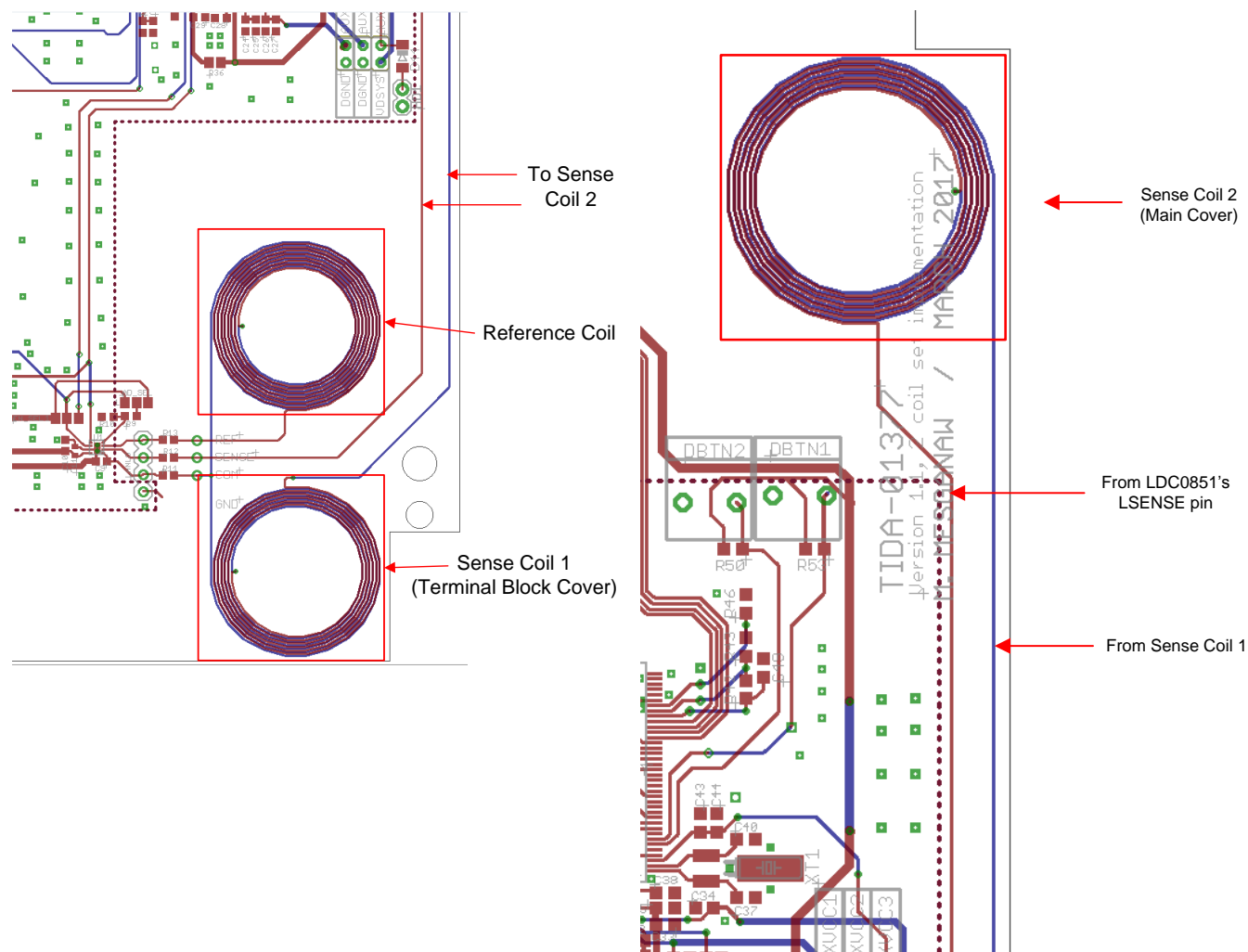


図 32. Reference and Sense Coil 1 of Two-Sense-Coil Implementation

図 33. Sense Coil 2 of Two-Sense-Coil Implementation

Note that the reference coil shown in 図 32 has more turns than the sense coils, which allows it to have a larger inductance to match the combined inductances of the sense coils. 表 5 lists the specifications of the reference coil.

表 5. Implemented Reference Coil Specifications for Two-Sense-Coil Implementation

PARAMETER	VALUE
Inner diameter( $d_{in}$ )	14.84 mm
Outer diameter( $d_{out}$ )	25 mm
$d_{in} / d_{out}$ constraint	$0.2 < d_{in} / d_{out} < 0.8$
$d_{in} / d_{out}$	0.59
Trace width (w)	10 mil
Spacing between traces (s)	10 mil
Number of turns on coil	Ten turns
Number of PCB layers	Two layers
Free-space inductance ( $L_{SENSOR}(d_{UPPER\_BOUND})$ )	9.799 $\mu$ H
ADJ <sub>CODE</sub>	14 (determined by tuning after initial board testing)



After designing first prototypes of the design, the final value for the  $ADJ_{CODE}$  was then iteratively determined by starting with an  $ADJ_{CODE}$  of 7 and then tuning the code as necessary. When tuning this value, if either the terminal block cover or the main cover is fully opened but the LDC0851 output is asserted high (erroneously indicating that tampering is not currently occurring), the  $ADJ_{CODE}$  is increased. If both the terminal block cover and the main cover are fully closed but the LDC0851 output is high (erroneously indicating that tampering is currently occurring), the  $ADJ_{CODE}$  is decreased. By following this process, an  $ADJ_{CODE}$  of 14 was found for the two-sense-coil variant.

### 3.4 Selecting Target Metal

Based on the designed PCB coils for the LDC0851, a few things must be kept into consideration for the target metal. First, when a target metal is brought into the magnetic field of the coil, the eddy currents on the surface of the metal flow in the lowest impedance path. The path taken is composed of concentric loops which match the shape of the coil and result in the eddy currents on the target metal mirroring the flow of current in the coil. The eddy currents on the conductive target mirror the flow of current in the sensors; therefore, the strongest target response is when the target covers the area of the coils because the image current path can better mirror the flow of current in the coils. If the target size is smaller than the sensor, the change in coil inductance from bringing the conductive target metal near the coils is reduced. As a result, the area of the target metal must be larger than the area of the PCB coil, as stated in 式 11.

$$AREA_{TARGET} > AREA_{COIL} \quad (11)$$

Like all AC currents, the eddy currents induced by the LDC0851 AC magnetic field flow near the surface of the conductor and reduce in amplitude deeper into the conductor. The attenuation of current follows an exponential trend with distance from the surface. The skin depth,  $\delta$ , is the distance at which the current is reduced to  $1/e$  ( $\approx 37\%$ ) of the density at the surface. Every additional increase of  $\delta$  from the surface sees an additional  $1/e$  reduction in current. A conductor with a thickness equal to one skin depth for a given frequency carries 63.2% of the current of an infinitely-thick conductor. With a conductor of three skin depths thick, 95% of the total current will be induced. To maximize the highest eddy current flow, and therefore also the change in inductance based on target movement, the ratio of the target thickness to skin depth must be large. A good general guideline is to ensure that the target thickness is at least three skin depths, as indicated in 式 12.

$$thickness_{TARGET} > 3 \times \delta_S \quad (12)$$

For highly conductive materials, such as metals, the skin depth  $\delta_s$  can be calculated by 式 13:

$$\delta_S = \sqrt{\frac{\rho}{\pi \mu f_{SENSOR}}} \quad (13)$$

where,

- $\mu$  is the magnetic permeability of the material, which is  $\mu_0$  ( $4\pi \times 10^{-7}$ ) multiplied by the relative permeability of the conductor,
- $\rho$  is the resistivity of the conductor,
- and  $f_{SENSOR}$  is the sensor frequency.

To calculate skin depth for different target metal materials, use the skin depth calculator tool in the inductive sensing design calculator spreadsheet (SLYC137) instead of manually calculating the skin depth using 式 13. As 図 34 shows, the skin depth calculator tool can calculate the skin depth based on the sensor frequency and the target material without requiring the designer to look up the values of  $\mu$  and  $\rho$ .

### Skin Depth Calculator

[Return to Main Page](#)

AC currents remain on the surface of conductor, decaying in an exponential manner. The depth of ~63% of the current is called the skin depth. A higher frequency will have a shallower skin depth. It is recommended to use a target thickness of at least 3 skin depths for a good LDC measurement. If you want to minimize the effect of a conductor, use a target thickness of less than 0.5 skin depths. Reminder: 1oz copper is ~35µm thick.

Target Material	Copper
Conductivity	16.7E-9 Ωm
Relative Permeability	1.00
Sensor Frequency	1.000 MHz
Skin Depth	65.1 µm
Material Thickness	0.80 mm
Number of Skin Depths:	12.29 skin depths
Percentage of Current:	100.000 %

$$\text{Skin Depth} = \delta_s = \sqrt{\frac{2\rho}{2\pi f \mu_0 \mu_r}}$$

where :

$\rho$  = bulk resistivity (ohm - meters)

$f$  = frequency (Hertz)

$\mu_0$  = permeability constant (Henries / meter) =  $4\pi \times 10^{-7}$

$\mu_r$  = relative permeability (usually ~ 1)

Courtesy of Microwaves101.com

### Quick Sensor L/C/f Calculator

L	20.000 µH
C	100.000 pF
fsensor	3.559 MHz

Spiral\_Inductor\_Designer LDC0851\_calc LDC2114\_Config\_tool LDC1101\_Calc Output Code Calculator SkinDepth S

図 34. Skin Depth Calculator Tool

式 13 shows that skin depth varies with the material and sensor frequency. Poorer conductors, such as carbon, have a larger value for their skin depth. The skin depth also becomes smaller and smaller at higher frequencies. As a result, the conductive target metal material matters less at high frequencies, as 図 35 shows.

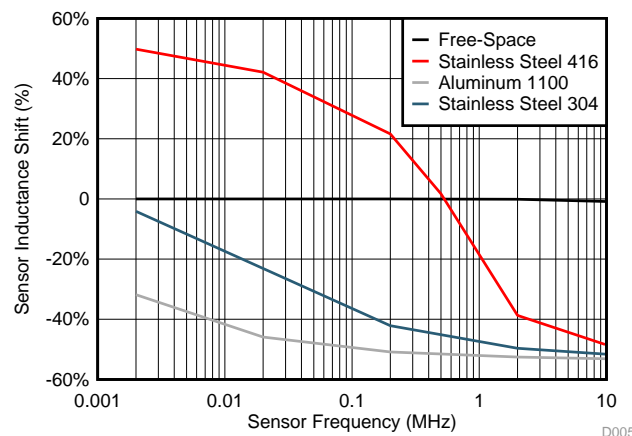


図 35. Sensor Inductance Shift versus Sensor Frequency for Conductive Target Metals

In addition to the dimensions of the target metal, another thing that to keep in consideration is that from a mechanical perspective the target material must be physically stable and exhibit uniform movement without warping or tilting.

For more details on target metal properties, see the application note for the LDC target design [2].

### 3.4.1 Utilized Target Metal

In this design, copper tape is used as the target metal because it is easy to install. Ideally, a material that is less malleable should be used in a final application because this leads to less variation in target metal-to-sense-coil distances across multiple boards. The area of the target metal is selected to be larger than the sense coil as mentioned in 式 11 so that the target metal can cover the entire area of the sensor coil. Based on the material type of the target metal (copper) and the minimum sensor frequency ( $f_{\text{SENSOR}(d_{\text{UPPER\_BOUND}})$ ), the skin depth calculator tool is used to calculate the value of three skin depths. This three-skin depth value is 49.34  $\mu\text{m}$  for the one-sense-coil implementation and 58.89  $\mu\text{m}$  for the two-sense-coil implementation, which are both much smaller than the thickness of the utilized copper tape. Based on 式 12, the copper tape has enough thickness to be used as the target metal.

In this design, the copper tape covers the entire platform, as 図 25 shows. To cover the entire area of the sensor coil, the left side of the copper tape begins on the platform and then expands past the platform so that the right side of the tape is left hanging. If the e-meter case can be modified, one potential improvement is to add a second platform so that the right side of the copper tape can connect to the second platform. This setup provides an easier method to ensure that the copper tape remains mechanically stable. In this design, the copper tape is made to remain relatively mechanically stable for the terminal block cover detection by wrapping the copper tape around the paper backing of the tape, which is relatively stable.

For the two-sense-coil implementation (see 図 31), the target metal for the main cover detection is extended by adding copper tape on the portion of the target metal that is secured by the standoffs. By adding this tape, the upper-left corner of the case is covered with the target metal so that the entire main cover sensor coil is covered by the target metal.

## 3.5 Reducing LDC0851 Current Consumption

### 3.5.1 Estimating LDC0851 Active Supply Current

The LDC0851 active supply current ( $I_{\text{DD}}$ ) is the sum of three components. The first component is the static current ( $I_{\text{STATIC}}$ ), which is the DC device current given in the electrical characteristics section of the LDC0851 data sheet and does not vary with frequency. This DC device current comes from the inductive switch core of the LDC0851, which is the portion in 図 36 that is highlighted red.

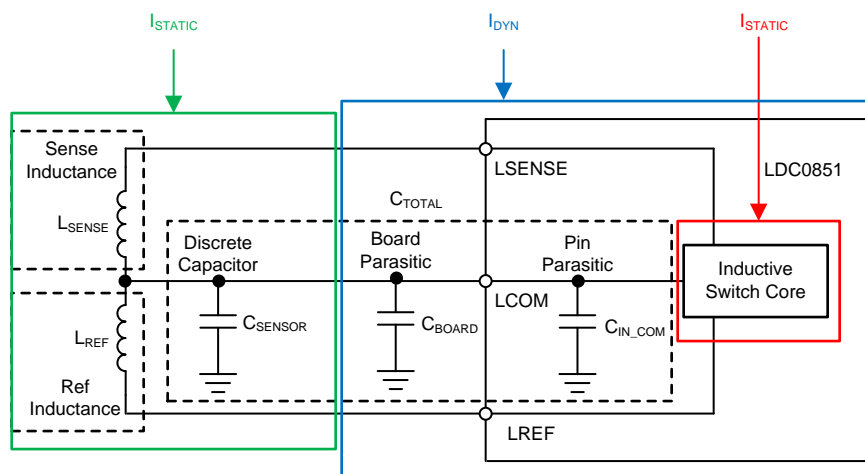


図 36. LDC0851 Active Current Consumption Components

The second current component is the dynamic current ( $I_{DYN}$ ). The dynamic current is the AC device current, which varies with both sensor frequency ( $f_{SENSOR}$ ) and the board parasitic capacitance  $C_{BOARD}$ ). The portion of the LDC0851 sensing circuitry that corresponds to the dynamic current is shown in 図 36 in blue. 式 14 shows the formula for the dynamic current.

$$I_{DYN} = 1.5 \times f_{SENSOR} \times C_{BOARD} + (24.262 \times 10^{-12} \times f_{SENSOR}) \quad (14)$$

The last component of the LDC0851 active current consumption is the sensor current ( $I_{SENSOR}$ ). The sensor current is the AC current required to drive the external LC sensor. This AC current varies both with frequency and the equivalent inductance of the sensor coils. 式 15 shows how to calculate the sensor current.

$$I_{SENSOR} = \frac{1}{17.1 \times L_{SENSOR} \times f_{SENSOR}} \quad (15)$$

By adding the three current-consumption components together, the active mode current consumption can be calculated as shown in 式 16.

$$I_{DD} = I_{DYN} + I_{STATIC} + I_{SENSOR} \quad (16)$$

式 14 and 式 15 show that there are different trends for the dynamic current and sensor current across frequency. If the sensor frequency increases, the dynamic current increases but the sensor current decreases. However, because the sensor current has a larger dependence on frequency, the active current consumption often follows a similar trend as the sensor current where increasing the frequency leads to a lower active current consumption.

### 3.5.2 Estimating LDC0851 Average Current Consumption

The active mode current consumption of the LDC0851 is relatively large, thus the LDC0851 device is only enabled long enough to get a valid reading from the LDC0851. By providing pulses to the enable pin of the LDC0851 device, the average current consumption of the LDC0851 can be greatly reduced. 図 37 shows an example pulse that can be provided on the LDC0851 enable pin. To reduce the average current consumption of the LDC0851 to be as small as possible, the pulse width ( $t_{PULSE}$ ) must be minimized as much as possible.

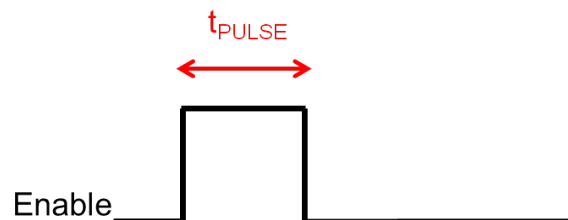


図 37. Enable Pulse

The minimum pulse width can be found by using 式 17.

$$t_{PULSE,min} = t_{AMT} + (2 \times t_{CONVERSION,max}) \quad (17)$$

where,

- $t_{AMT}$  is the necessary time to go from shutdown mode to active mode, which is defined in the LDC0851 data sheet (SNOSCZ7A) to be 450  $\mu s$ ,
- $t_{CONVERSION,max}$  is dependent on the minimum frequency of the sensor as shown in 式 18.

$$t_{\text{CONVERSION, max}} = \frac{1}{231 \times 10^{-6} \times f_{\text{SENSOR, min}}} \quad (18)$$

The minimum frequency of the sensor corresponds to the sensor frequency when the target metals are the furthest away from the sense coils. After calculating the minimum sensor frequency,  $t_{\text{CONVERSION, max}}$  and  $t_{\text{pulse, min}}$  can be calculated. For valid readings of the LDC0851 output, regardless of the distance from the sense coil to target metal, the selected pulse width must at least be greater than  $t_{\text{pulse, min}}$ , as shown in 式 19.

$$t_{\text{PULSE}} \geq t_{\text{PULSE, min}} \quad (19)$$

After calculating the selected pulse width, the time the LDC0851 is actually ON can be calculated by using 式 20.

$$t_{\text{ON}} = t_{\text{PULSE}} \quad (20)$$

Based on the calculated values of ON time and the LDC0851 active current consumption, the average current consumption of the LDC0851 can be approximated by averaging the current shown in 図 38 across time.

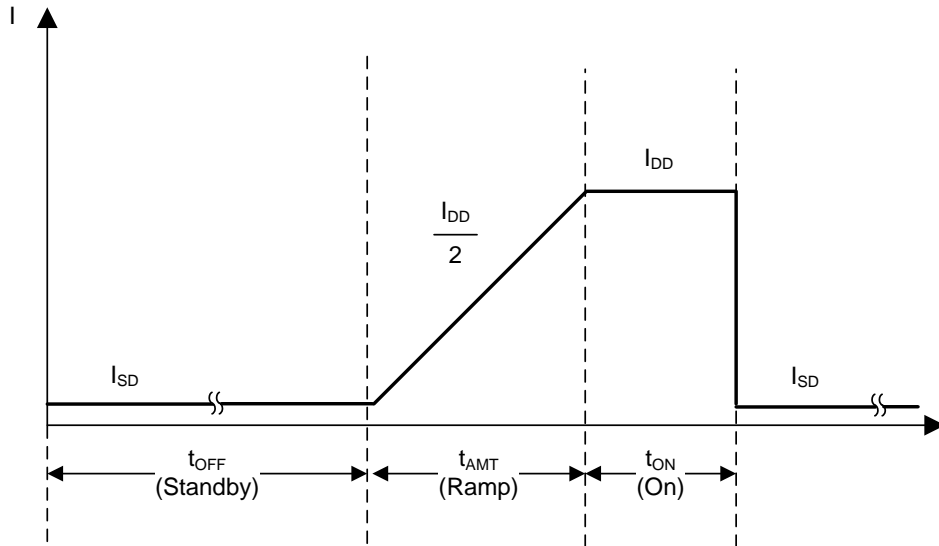


図 38. Estimate of LDC0851 Average Current Consumption

This total average current can be calculated by using 式 21.

$$I_{\text{AVG}} = I_{\text{ON}} + I_{\text{RAMP}} + I_{\text{OFF}} \quad (21)$$

where,

- $I_{\text{ON}}$  is the average active current given from 式 22,
- $I_{\text{RAMP}}$  is the average ramp current approximated from 式 23,
- $I_{\text{OFF}}$  is the average standby current from 式 24.

$$I_{\text{ON}} = f_{\text{Sample}} \times t_{\text{ON}} \times I_{\text{DD}} \quad (22)$$

where,

- $f_{\text{Sample}}$  is the number of times the LDC0851 is sampled in a second (a sample rate of 1 Hz is used in this application because tamper detection does not require a fast sample rate to detect).

$$I_{\text{RAMP}} \approx f_{\text{Sample}} \times t_{\text{AMT}} \times \frac{I_{\text{DD}}}{2} \quad (23)$$

$$I_{OFF} = (1 - f_{Sample} \times (t_{pulse})) \times (I_{SD}) \quad (24)$$

Based on 式 21, the average current consumption range can be determined by calculating the average current consumption for two cases: one where the target metals are the closest to the sense coil and the other case where the metals are the furthest from the sense coil. For these two scenarios, there are two different values for the sensor frequency and inductance, which in turn cause different values for the average current consumption; however, the pulse width parameter must be the same for both scenarios. Instead of using 式 21 to calculate the average current consumption for these two conditions, a simpler option is to use the battery life calculator excel tool (located within the software package) shown in 図 39.

## Battery Life Calculator Excel Tool

	A	B	C	D	E	F	G	H
1	Battery Capacity	220	mAh					
2	fsensor	15.66437815	MHz					
3	Sensor Inductance	4.801484	uH					
4	Sample Rate	1	sps					
5	Board Parasitic Capacitance	4	pF					
6	Pulse Width	0.001068115	seconds					
7	lifetime	14.1	years	Equation 14: Battery Lifetime (years) = $\frac{\text{Battery Capacity}}{I_{AVG}}$				
8	iaverage	1.8	uA					
9								
10								
11								
12	C <sub>board</sub>	4	pF	Estimated from PCB trace				
13	I <sub>static</sub>	0.0007	A	Given in electrical table as 0.7mA				
14	I <sub>dyn</sub>	0.000474035	A	Equation 4: $I_{dyn} = (24.262 \cdot 10^{-12}) \cdot f_{SENSOR} + 1.5 \cdot f_{SENSOR} \cdot C_{BOARD}$				
15	I <sub>sensor</sub>	0.000777527	A	Equation 5: $I_{sensor} = \frac{1}{17.5 \cdot I_{SENSOR} \cdot f_{SENSOR}}$				
16	I <sub>DD</sub>	0.001951562	A	Equation 6: $I_{DD} = I_{dyn} + I_{static} + I_{sensor}$				
17	I <sub>SD</sub>	0.00000014	A	Given in electrical table as typ 0.140uA				
18	I <sub>TPL</sub>	0	A	Given in datasheet as 35nA				
19								
20	t <sub>ΔMT</sub>	0.00045	sec	Given in datasheet as 450μs				
21								
22	t <sub>CONV</sub>	0.00027636	sec	$t_{CONVERSION} = \frac{1}{231.0 \times 10^{-6} \cdot f_{SENSOR}}$				
23								
24	I <sub>ON</sub>	1.20629E-06	A	Equation 10: $I_{ON} = f_{sample} \cdot (2 \cdot t_{CONVERSION}) \cdot (I_{DD} + I_{TPL})$				
25	I <sub>RAMP</sub>	4.39101E-07	A	Equation 11: $I_{RAMP} = f_{sample} \cdot (t_{ΔMT}) \cdot (\frac{I_{DD}}{2} + I_{TPL})$				
26	I <sub>OFF</sub>	1.3985E-07	A	Equation 12: $I_{OFF} = (1 - f_{sample} \cdot (t_{ΔMT} - 2 \cdot t_{CONVERSION})) \cdot (I_{SD} + I_{TPL})$				
27								
28	I <sub>AVG</sub>	1.78524E-06	A	Equation 13: $I_{AVG} = I_{ON} + I_{RAMP} + I_{OFF}$				

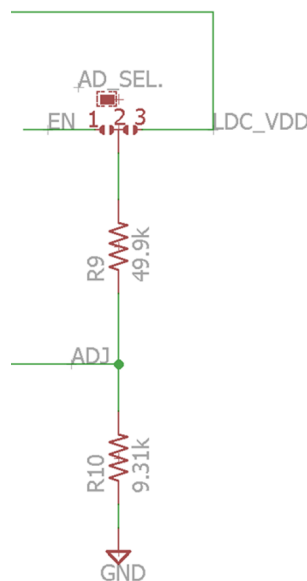
図 39. Modified Battery Life Calculator Excel Tool

To use the battery life calculator tool to calculate the average current consumption for when the target metal is the closest and furthest from the sense coil, the parameters of the system can be plugged into the orange cells. For the two different scenarios, the same pulse width is used, which must be at least greater than  $t_{pulse,min}$ , as stated in 式 19. The only parameters that vary for the two scenarios are the sensor frequency and inductance.

The battery life calculator tool can also be used to tweak the different parameters of the design to try to minimize the average current consumption. This tool is helpful because modifying some system parameters may not always have the same effect. For example, reducing the base sensor inductance may cause a larger active current consumption, which may sometimes cause a larger average current consumption; however, reducing the sensor inductance also causes a larger sensor frequency, which leads to a smaller minimum pulse width that other times may cause a smaller average current consumption, despite having a larger active current consumption. Using the modified battery life calculator tool to try to reduce the average current consumption is a good way to see how tweaking the system parameters affects the average current consumption for various conditions.

### 3.5.3 Low Power Generation of ADJ Voltage

To select a particular  $ADJ_{CODE}$ , a specific voltage must be provided on the ADJ pin of the LDC0851. This voltage is commonly generated by a voltage divider that uses two resistors and VCC to generate the ADJ voltage. For the one-sense-coil implementation of this design, an  $ADJ_{CODE}$  value of four is generated (for the two-sense-coil implementation, R10 is replaced with a 44.2-k resistor to create an  $ADJ_{CODE}$  value of 14) using the resistor dividers shown in 40.



40. ADJ Resistors

For a VCC voltage of 3.3 V, approximately 56  $\mu$ A flows through the resistors. If these resistors are powered from VCC, this 56- $\mu$ A current is constantly drawn from the supply. When the LDC0851 device is enabled, this 56- $\mu$ A current consumption is relatively small compared to the active current consumption of the LDC0851 (in the mA range); however, when the LDC0851 device is disabled, this current is relatively large compared to the small shutdown current (in the nA range) of the LDC0851. As a result, the current consumption when the LDC0851 device is disabled is dominated by the current flowing through the ADJ resistors, which leads to a high average current consumption.

To reduce the average current consumption, the ADJ resistors in this design are powered from the enable pin instead of VCC. Using this configuration allows relatively negligible current to flow through the resistors when the LDC0851 device is enabled and no current flows through the resistors when the LDC0851 device is disabled. The voltage at the ADJ pin is only required to be present when the LDC0851 is enabled; the functionality of the LDC0851 is not affected when the voltage at the ADJ pin is not present and when the LDC0851 is disabled. So by connecting the ADJ resistors to enable, the average current consumption from the current flowing through the ADJ resistors becomes negligible.

### 3.5.4 Tweaking System Parameters to Reduce Average Current Consumption

Using the battery life calculator tool, the system parameters are tweaked to reduce the current consumption. Use of the tool for this design led to the discovery that the average current consumption can be reduced by increasing the sensor frequency while keeping the sensor inductance fixed. If the sensor inductance is increased, based on 式 5, an increase in sensor frequency can only be achieved by decreasing the total capacitance  $C_{SENSOR}$ ). This total capacitance is reduced specifically by reducing the



value of  $C_{\text{SENSOR}}$ . In this design,  $C_{\text{SENSOR}}$  has been decreased from the 62-pF value recommended by WEBENCH down to 27 pF. By replacing the  $C_{\text{SENSOR}}$  with a smaller capacitance, the total capacitance is reduced to 43 pF. This 43 pF is greater than the 33-pF minimum total capacitance constraint. In addition, this capacitance results in a  $f_{\text{SENSOR}}(d_{\text{LOWER\_BOUND}})$  value that is 16.656 MHz for the one-sensor-coil variant, a  $f_{\text{SENSOR}}(d_{\text{UPPER\_BOUND}})$  value of 15.665 MHz for the one-sensor-coil variant, and a  $f_{\text{SENSOR}}(d_{\text{UPPER\_BOUND}})$  value of 10.996 MHz for the two-sense-coil variant, which are all still less than the 19-MHz maximum  $f_{\text{SENSOR}}$  constraint. As a result, changing  $C_{\text{SENSOR}}$  to 27 pF is a valid change.

Based on the new minimum sensor frequency of 15.665 MHz for the one-sense-coil variant from replacing  $C_{\text{SENSOR}}$ ,  $t_{\text{CONVERSION,max}}$  is calculated to be 276  $\mu\text{s}$  for the one-sense-coil variant. This value of  $t_{\text{CONVERSION,max}}$  in turn causes a  $t_{\text{PULSE,min}}$  value equal to 1.003 ms. For the two-sense-coil variant, the new minimum sensor frequency of 10.996 MHz results in a  $t_{\text{CONVERSION,max}}$  value of 394  $\mu\text{s}$ . This value of  $t_{\text{CONVERSION,max}}$  in turn causes a  $t_{\text{PULSE,min}}$  value equal to 1.237 ms. Based on the value of  $t_{\text{PULSE,min}}$ , the MSP430 MCU is configured to provide a pulse on the LDC0851 enable pin that is slightly larger than the corresponding  $t_{\text{PULSE,min}}$  value.

To reduce the average current consumption of the LDC0851, the sample rate of the LDC0851 ( $f_{\text{SAMPLE}}$ ) is selected to be a low value of 1 Hz. This low sample rate suffices for many systems because the process of meter tampering is a relatively slow process.

### 3.6 Software Implementation

The major peripherals of the MSP430F67791A that are used in this design are the auxiliary power supply module (AUX), real-time clock (RTC), liquid-crystal display (LCD), timers (timer 3 and timer 0), port pins, and clock system. After the peripherals have been set up, the MSP430 MCU enters LPM3 mode and waits for timer interrupts to properly read the LDC0851 device and handle periodic tasks.

#### 3.6.1 AUX Module

The AUX module is set so that hardware switching is enabled for DVCC and AUXVCC2. AUXVCC1 is disabled. In the software, the SVSMH voltage is set to level 5; see the [MSP430F67791A](#) data sheet (SLAS983) for the range of exact voltages that correspond to this particular level). When VDSYS, the supply selected to power the chip, falls below this SVSMH level, the AUX module triggers for VDSYS to switch to another supply (as long as the supply to switch to is above a user-defined threshold). The OK-voltage threshold for AUXVCC2 (AUX2LVL) is level 5. The OK-voltage level for DVCC (AUX0LVL) is level 6. Note that if DVCC was previously not declared OK, but is later on, the AUX module switches to DVCC even if VDSYS is not below the SVSMH level. This auto-switch behavior is only true for DVCC and is not applicable for AUXVCC1 or AUXVCC2.

Whenever the supply powering the chip is switched from DVCC to AUXVCC2 or vice versa, the AUX module is configured to generate an interrupt to log this change.

For more information about the AUX module used in this design, see the user's guide or the following TI design: [TIDM-AUX-MODULE](#).

#### 3.6.2 Real Time Clock (RTC\_C)

The RTC\_C is an RTC module that is configured to keep track of the time and date. This module is used to detect when the number of seconds defined in the "WAIT\_TIME" macro in *board.h* have elapsed since the microcontroller has been reset. Until the number of seconds defined in the "WAIT\_TIME" macro has passed, the case tamper detection functionality is disabled. This macro enables opening the meter case, programming the MSP430, and having enough time for the case to be closed without registering opening the case for programming the MSP430 as a case tamper event.

The RTC\_C module is also used to log the time of the first case tamper event detected on RTCCAP1, which is connected to the LDC0851 output. To clear the current tamper event and allow detection of the next tamper event, DBTN1 can be pressed whenever DVCC is available.

### 3.6.3 LCD Controller (LCD\_C)

The LCD controller on the MSP430F67791A can support up to eight-mux displays and 320 segments. The LCD controller is also equipped with an internal charge pump that can be used for good contrast. In the current design, the LCD controller is configured to work in four-mux mode using 160 segments with a refresh rate set to ACLK/64, which is 512 Hz.

### 3.6.4 Timer3

When the MCU is in LPM3 low power mode, the Timer3 timer is used to wake up the MCU to perform routine tasks. Timer3 uses the 32.678-KHz ACLK clock as the clock designated for counting. This ACLK clock is enabled when the device is in LPM3 mode, which allows the timer to properly count and wake up the MCU from LPM3 mode. Timer3 is configured in up/down mode to generate an interrupt four times per second. [Figure 41](#) shows the code executed in the Timer3 interrupt service routine (ISR).

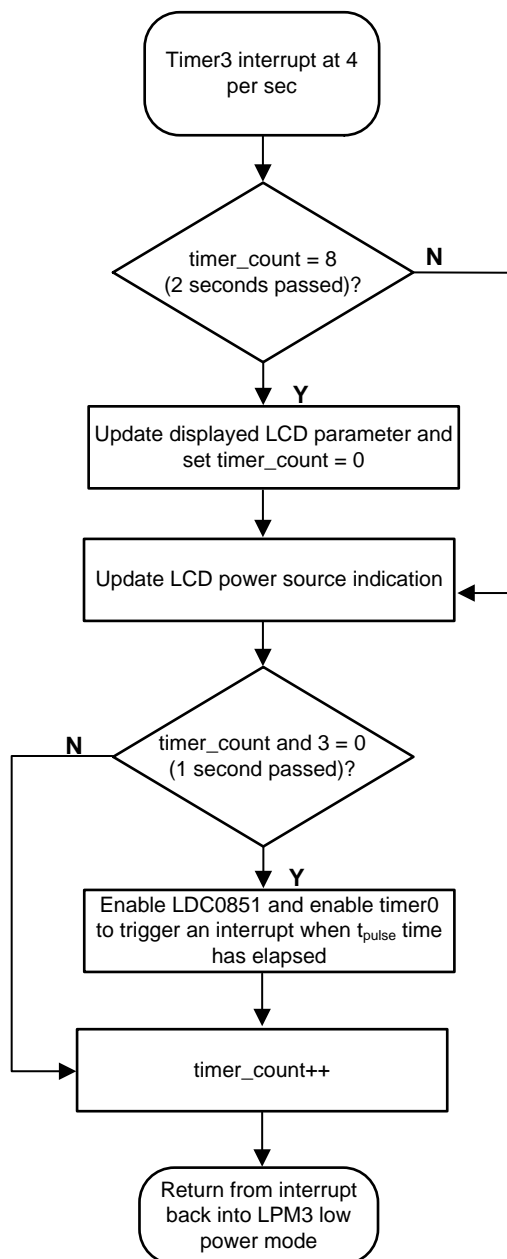


図 41. Timer3 ISR

Whenever a Timer3 interrupt occurs, the symbol on the LCD that is used to indicate the power source of the system (either DVCC or AUXVCC2) is updated to reflect any power supply switching that has occurred.

In the Timer3 ISR, there is a *timer\_count* variable that keeps track of how many times the timer3 interrupt has occurred. This variable is used to determine when to run one-second tasks and two-second tasks. When this variable has a value of 8, then it is time to run the two-second tasks. These two-second tasks include resetting the *timer\_count* variable and updating the LCD to display a new parameter.

When the timer\_count variable has a value of either of 4 or 8, it is time to run the one-second tasks. This one-second task includes enabling the LDC0851 and enabling the Timer0 interrupt, where Timer0 is used to ensure that the LDC0851 is enabled for the proper amount of time before reading the LDC0851 output. After enabling the timer0 timer, the code exits the Timer3 ISR and the MCU goes back to LPM3 until the timer0 interrupt occurs.

### 3.6.5 Timer0

Timer0 is used to provide the necessary pulse width on the LDC0851 enable pin. Because  $t_{\text{PULSE,min}}$  is different for the one-sense-coil- and two-sense-coil variants, there are macros in the *board.h* file in the code that select which board is being used to select the proper value of  $t_{\text{PULSE,min}}$ .

The LDC0851 is actually enabled in the Timer3 ISR. Timer3 triggers Timer0 so that after the LDC0851 is first enabled, the LDC0851 continues to be enabled for a total time equal to the desired enable pulse width.

Timer0 uses the 32.678-KHz ACLK clock as the clock designated for counting. This ACLK clock is enabled when the device is in LPM3 mode, which allows the timer to properly count and wake up the MCU from LPM3 mode when it is time to read then disable the LDC0851. The value that timer0 actually counts to is able to compensate for the time it takes for the device to exit LPM3 and enter the timer0 ISR so that the pulse width on the LDC0851 enable pin is generated as desired. Timer0 is also configured in up mode to generate a single interrupt every time it is triggered by Timer3. [Figure 42](#) shows the code executed in the Timer0 ISR.

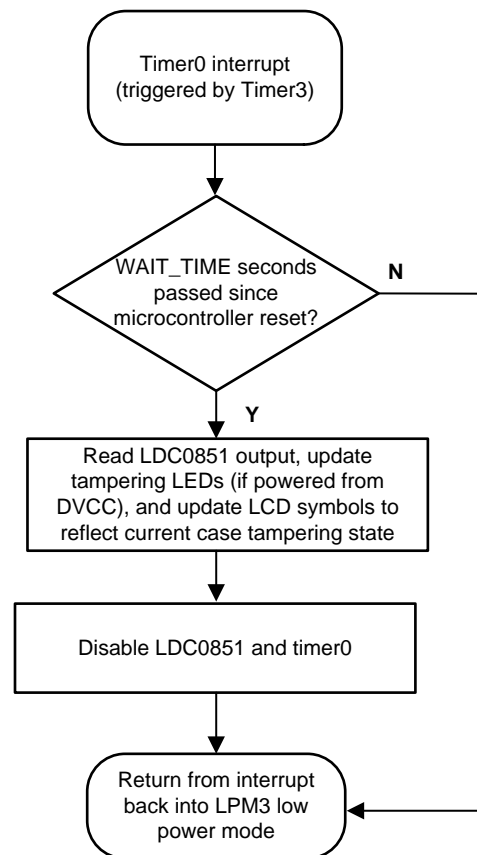


図 42. Timer0 ISR

In the Timer0 ISR, before reading the LDC0851, it is determined if "WAIT\_TIME" seconds have passed since the MSP430 was first reset. This check is done so that the case can be opened, the MSP430 programmed, and then the case closed without the MSP430 registering this as a tamper event. The actual counting to WAIT\_TIME seconds is done by the RTC. After the RTC has counted to WAIT\_TIME seconds, a flag is asserted that allows the Timer0 ISR to start reading the LDC0851 output and enable case tamper detection.

After reading the LDC0851 output, the LCD symbols that are used to indicate case tampering are updated. These symbols update regardless of whether the board is powered by DVCC or AUXVCC2. If the board is powered from DVCC, which is used to power the board LEDs, the LEDs on the board are also updated to indicate the current case-tampering status.

After the LCD is updated to reflect the most recent tamper status, the LDC0851 is disabled. In addition, timer0 is disabled until the next time timer3 enables it. The code then exits the timer0 ISR and goes back to LPM3 mode until the next timer3 interrupt.

## 4 Getting Started Hardware and Software

### 4.1 Hardware

The following images show the PCB within the meter case. For the one-sense-coil variant, [Figure 43](#) shows the top view of the PCB and [Figure 44](#) shows the location of various pieces of the system based on functionality.

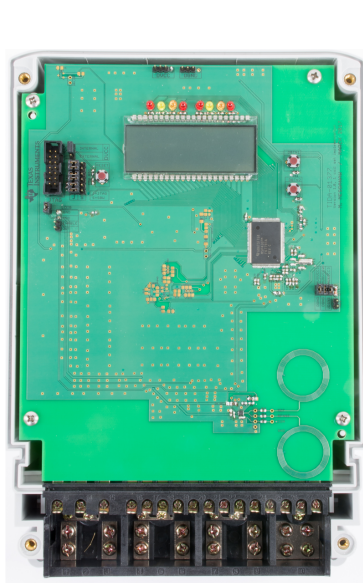


Figure 43. TIDA-01377 PCB One-Sense-Coil Variant Top View

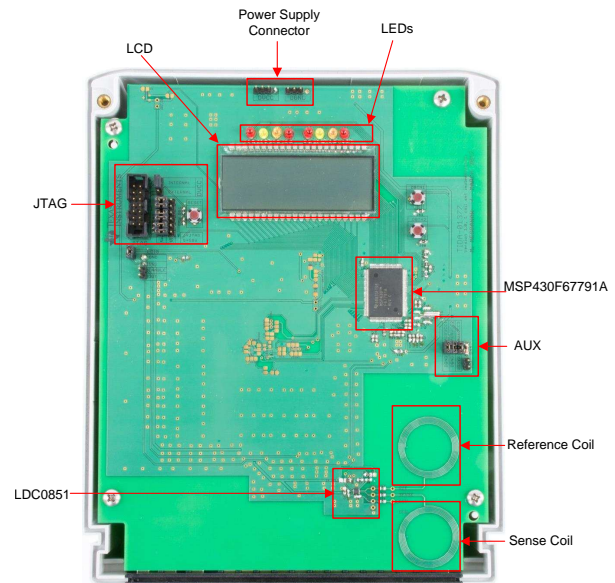


Figure 44. TIDA-01377 One-Sense-Coil Variant PCB With Components Highlighted—Top View

For the two-sense-coil variant, [Figure 45](#) shows the top view of the PCB and [Figure 46](#) shows the location of various pieces of the system based on functionality.

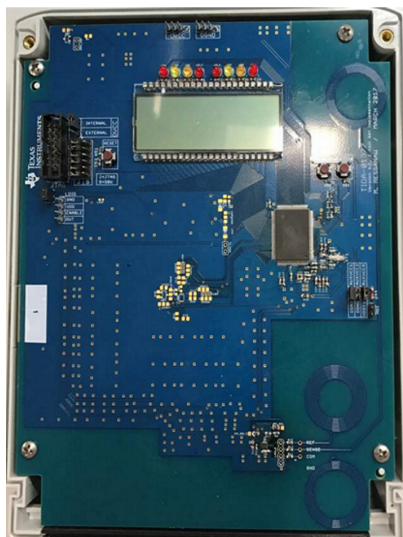


Figure 45. TIDA-01377 PCB Two-Sense-Coil Variant Top View

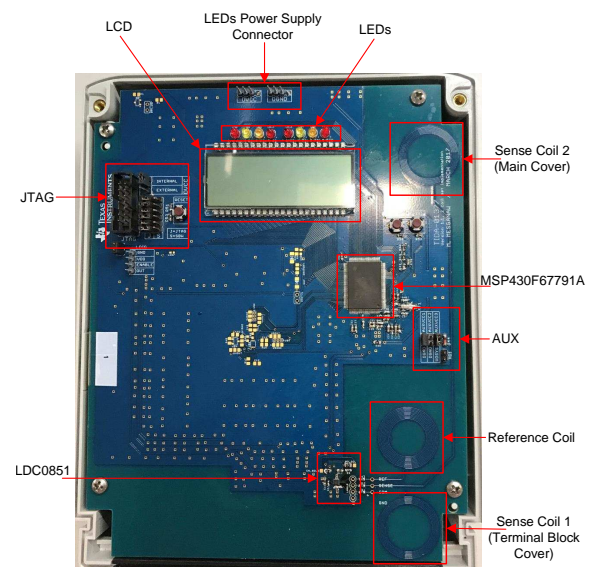


Figure 46. TIDA-01377 Two-Sense-Coil Variant PCB With Components Highlighted—Top View



### 4.1.1 Power Supply Options and Jumper Settings

A single DC voltage rail (DVCC) powers the majority of the board including the MSP430. DVCC can be derived either through JTAG or external power. If DVCC goes away, then the design is configured to switch automatically to an alternative power supply connected to AUXVCC2. The LDC0851 can be powered either separately from the rest of the board or using the same voltage rail used to power the MSP430 (either DVCC or AUXVCC2).

Various jumper headers and jumper settings are present to add to the flexibility of the board. Some of these headers require that jumpers be placed appropriately for blocks to function correctly. 表 6 shows the functionality of each jumper on the board and the associated functionality.

**表 6. Header Names and Jumper Settings**

HEADER OR HEADER OPTION NAME	TYPE	MAIN FUNCTIONALITY	ADDITIONAL COMMENTS
AD_SEL	Three-pad jumper resistor footprint	ADJ voltage divider power source	This option selects the power source for the ADJ resistor divider used to provide the proper voltage on the ADJ pin of the LDC0851. There are two options. Place a 0-Ω resistor between the center pad and pad 1 to generate the ADJ voltage from the LDC0851 enable. Place a 0-Ω resistor between the center pad and pad 3 to generate the ADJ voltage from the LDC0851 VDD supply. To reduce average current consumption, by default the jumper resistor is placed at pad 1.
AUXVCC1	Two-pin header(part of SV1 3x2 header)	AUXVCC1 selection and external power	Place a jumper here to connect AUXVCC1 to GND. This jumper must be present in this design because AUXVCC1 is disabled in the software. This two-pin header is a part of the SV1 3x2 header.
AUXVCC2	Two-pin header(part of SV1 3x2 header)	AUXVCC2 selection and external power	Place a jumper here to connect AUXVCC2 to GND. This jumper must be present if AUXVCC2 is not used as a backup power supply. If AUXVCC2 is used to provide a backup power supply to the MSP430™ MCU, connect the alternative power supply to this header. The software is configured to automatically switch to the supply connected to this header if power at DVCC is removed and the AUXVCC2 voltage is above a minimum threshold (see 3.6.1 for more details). This two-pin header is a part of the SV1 3x2 header.
AUXVCC3	Two-pin header(part of SV1 3x2 header)	AUXVCC3 selection	Place a jumper here to connect AUXVCC3 to VDSYS so that the RTC can be powered by whichever supply powers the chip. For this design, placing this jumper is necessary unless AUXVCC3 is powered from HD1. This two-pin header is a part of the SV1 3x2 header.
DGND	Header	Ground voltage header	Connect negative terminal of bench or external power supply here when powering the board externally.
DVCC	Header	VCC voltage header	Connect positive terminal of bench or external power supply here when powering the board externally.
EN_SEL	Three-pad jumper resistor footprint	LDC0851 enable select	This option selects the enable source for the LDC0851. There are two options. Place a 0-Ω resistor between the center pad and pad 1 to connect the LDC0851 enable to its VCC so that it is constantly ON. Place a 0-Ω resistor between the center pad and pad 3 so that the enable pin is connected to a microcontroller that can enable and disable the LDC0851 appropriately. To reduce average current consumption, by default the jumper resistor is placed at pad 3.
HD1	Header	AUXVCC3 external power	If the RTC is to be powered from a separate power source than the MSP430™ MCU or LDC0851, connect the external power supply here.
J	Jumper header option	4-wire JTAG programming option	Place jumpers at the J-header options of all of the six JTAG communication headers to select four-wire JTAG.
LANLG	Header	GND, LCOM, LSENSE, and LREF	This header can be used to view the LCOM, LSENSE, and LREF waveforms for internal debugging.

**表 6. Header Names and Jumper Settings (continued)**

HEADER OR HEADER OPTION NAME	TYPE	MAIN FUNCTIONALITY	ADDITIONAL COMMENTS
LDC_PWR	Header	LDC0851 power selection	Place a jumper here to power the LDC0851 from the supply used to power the MSP430™ MCU. Remove this jumper if the LDC0851 is to be powered from a separate power supply. The current consumption of the LDC0851 can also be measured by probing across this header.
LDIG	Header	LDC0851 power supply, enable, and output	To connect an external supply to the LDC0851, place the external supply between the GND and LDC_VCC pins of this header. This header can also be used to probe the LDC0851 enable and output pins.
S	Jumper header option	SBW JTAG programming option	Place jumpers at the S-header options of all of the six JTAG communication headers to select SBW JTAG.

#### 4.1.2 LEDs and Buttons

The TIDA-01377 design features two buttons and eight light-emitting diodes (LEDs). 表 7 and 表 8 show the functionality of these buttons and LEDs.

**表 7. Button Functionality**



BUTTON NAME	DESCRIPTION
DBTN1	Pressing this button clears the first case tampering event so that the next case tamper event is logged as the "first" case tamper event.
DBTN2	Not used

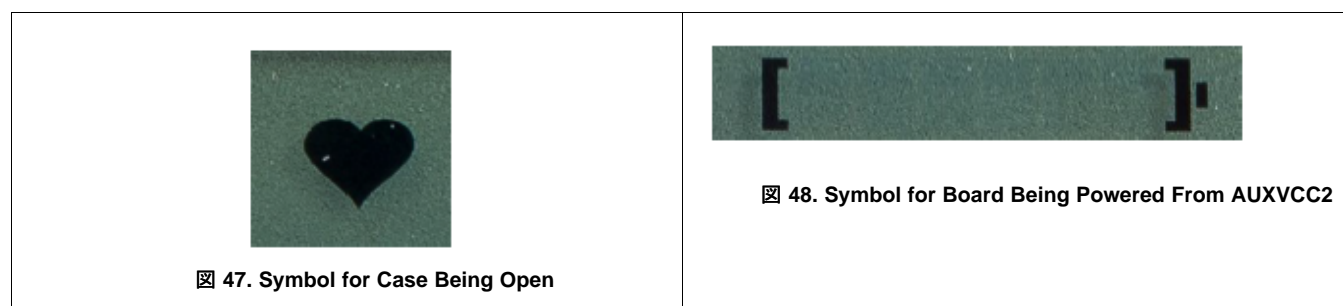
**表 8. LED Functionality**

LED NAME	DESCRIPTION
LED_A	When the board is powered by DVCC and "WAIT_TIME" seconds have elapsed, this LED is ON if there is currently a case tamper event (the case is currently opened). If the case is later closed, then this LED turns OFF.
LED_B	Not used
LED1	When the board is powered by DVCC, this LED is ON if a case tamper event occurred sometime after the "WAIT_TIME" seconds have elapsed and after the MSP430™ MCU was first reset. If this LED is OFF, then no tamper event has occurred. If the case is later closed, this LED stays ON unless the MSP430™ MCU is reset.
LED2	This LED is used to indicate that "WAIT_TIME" seconds have not passed since the MSP430™ MCU has first been reset. For every second this LED toggles states until "WAIT_TIME" seconds have elapsed. After "WAIT_TIME" seconds have passed, this LED turns OFF.
LED3	Not used
LED4	Not used
LED5	Not used
LED6	Not used



### 4.1.3 LCD

The LCD is used to display the current status of case tampering as well as the date and time of the first tamper attack. For each parameter that shows on the LCD, two items always display on the screen: a text and symbol combination to denote the parameter that is being displayed and the actual value of the parameter. In addition to the three items always on display, special characters also display on the LCD whenever the case is currently opened and the device is powered from AUXVCC2.  and  show the symbols corresponding to these statuses.



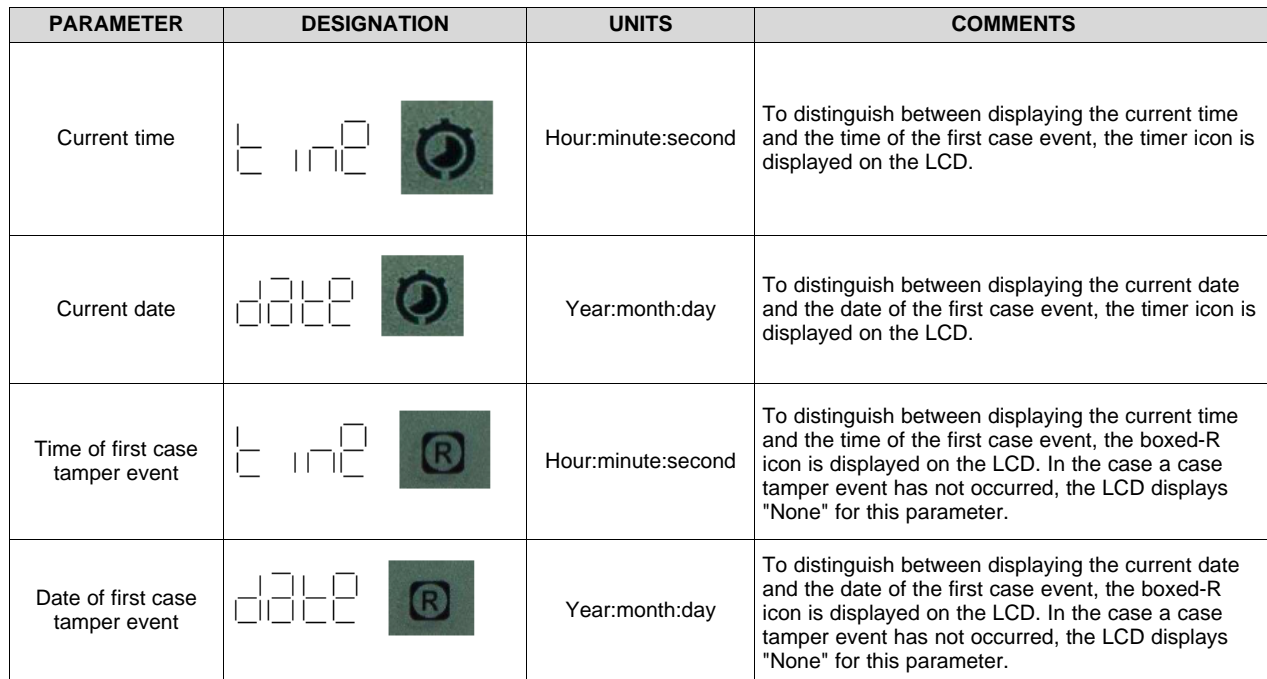




The bottom line of the LCD is used to denote the value of the parameter being displayed. The text to denote the parameter being shown displays on the top line of the LCD.  shows the different parameters that are displayed on the LCD and the associated units in which they are displayed. The DESIGNATION column shows which characters correspond to which metering parameter.

表 9. LCD Display Parameters

PARAMETER	DESIGNATION	UNITS	COMMENTS
Current time	time 	Hour:minute:second	To distinguish between displaying the current time and the time of the first case event, the timer icon is displayed on the LCD.
Current date	date 	Year:month:day	To distinguish between displaying the current date and the date of the first case event, the timer icon is displayed on the LCD.
Time of first case tamper event	time 	Hour:minute:second	To distinguish between displaying the current time and the time of the first case event, the boxed-R icon is displayed on the LCD. In the case a case tamper event has not occurred, the LCD displays "None" for this parameter.
Date of first case tamper event	date 	Year:month:day	To distinguish between displaying the current date and the date of the first case event, the boxed-R icon is displayed on the LCD. In the case a case tamper event has not occurred, the LCD displays "None" for this parameter.

## 4.2 Software

The source code is developed in the IAR™ environment using IAR compiler version 6.x. Earlier versions of IAR cannot open the project files. When the project is loaded in IAR version 6.x or later, the integrated development environment (IDE) prompts the user to create a backup. Click the **YES** button to proceed.

After opening the project, open the *board.h* file and configure the "WAIT\_TIME" macro to the desired wait time (in seconds) before registering tamper events. This macro is used to provide enough delay after programming the MSP430 to close the case before it is registered as a tamper event. After configuring the "WAIT\_TIME" macro, the proper variant of the board must be selected. If the software is to be flashed onto the one-sense-coil variant of the design, make sure that the "ONE\_COIL\_IMPLEMENTATION" macro in this file is enabled and the "TWO\_COIL\_IMPLEMENTATION" macro is disabled. If the software is to be flashed onto the two-sense-coil variant of the design, make sure that the "TWO\_COIL\_IMPLEMENTATION" macro is enabled and the "ONE\_COIL\_IMPLEMENTATION" macro is disabled. After making these changes to the *board.h* file, compile the IAR project.

To compile the IAR project for this design, open the *TIDA-01377.eww* workspace in IAR, right click the TIDA-01337 project, select *Rebuild All* (see [Figure 49](#)), and then download this project onto the MSP430F67791A device.

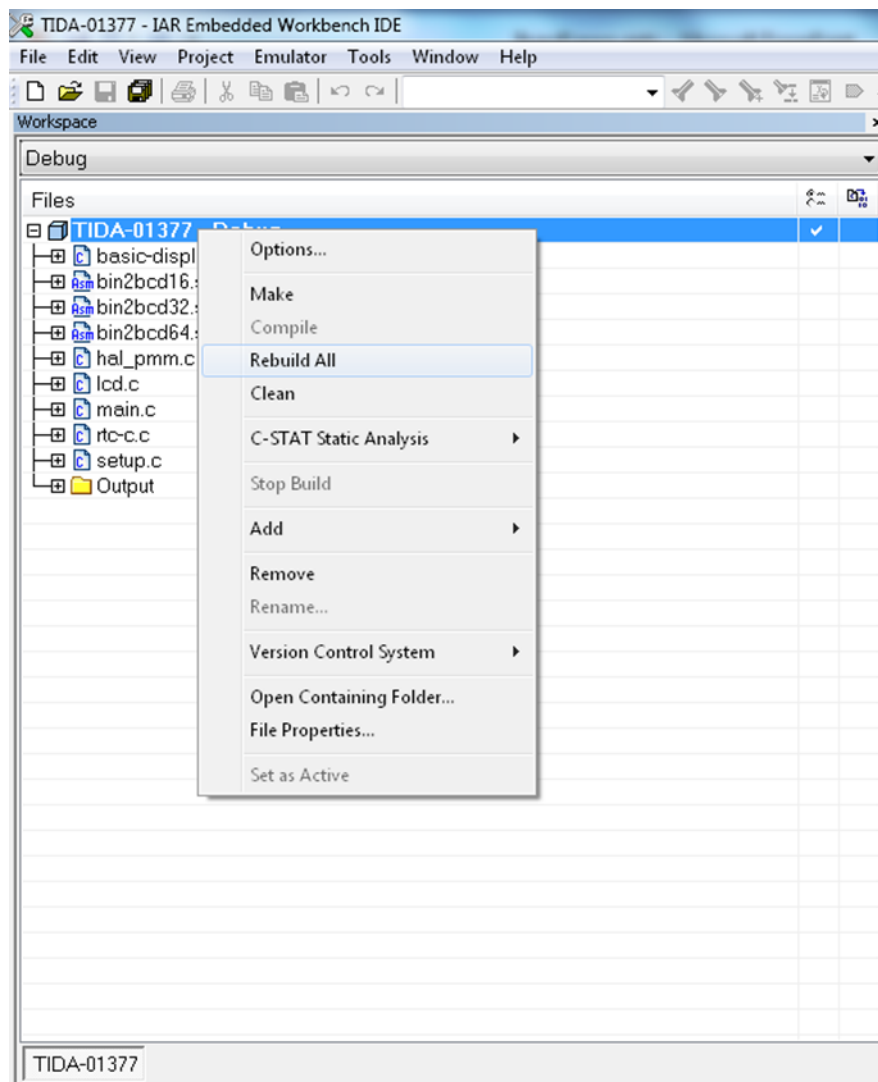


図 49. TIDA-01377 Project Compilation

## 5 Testing and Results

### 5.1 Case Tamper Detection Functionality Testing

To test the basic functionality of this design for the one-sense-coil implementation, the terminal block cover was placed on the main cover and screwed down. Then after "WAIT\_TIME" seconds had passed, the terminal block cover was unscrewed and removed from the top of the main cover. While removing the cover, the tampering LEDs were monitored to determine if case tampering has been properly detected. In addition, to verify that the LDC0851 was not affected by a strong DC magnet, a 1.3-T cylindrical magnet with 63.5-mm diameter and 25.4-mm thickness was applied above the LDC0851 sensing circuitry.

The same set of tests were also performed on the two-sense-coil implementation, including the additional test of opening the main cover with the terminal block cover completely closed to verify that this tampering event was detected.

In both variants of this design, the design was able to properly detect case tampering. Both implementations detected the opening of the terminal block cover when the terminal block cover was approximately 1 mm to 2 mm from its closed position. For the two-sense-coil implementation, an opening as small as 4 mm was accurately detected.

In addition, the design was not affected by the strong DC magnet applied. A video of the testing can be found within the following training module: [TIDA-01377 Demo Video](#).



### 5.2 LDC0851 Average Current Consumption Testing

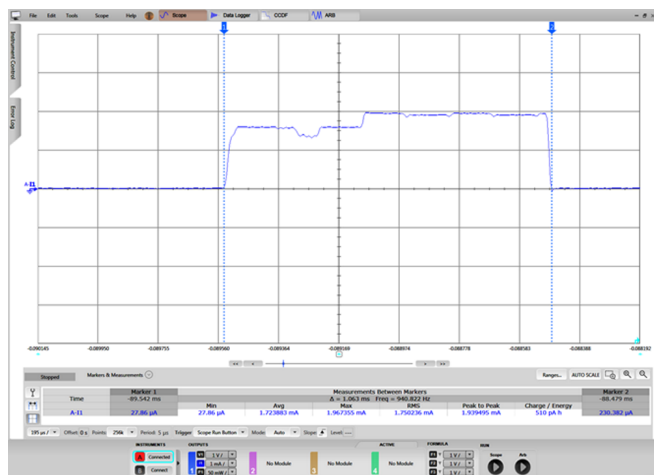
Because the power to the LDC0851 is duty cycled, using a multimeter to measure the current consumption does not provide accurate readings for the average current. As a result, a power analyzer was used to measure the average current consumption. The power analyzer works by acting as an external power source and measuring the current consumption drawn from that which it powers.

For this test, two different supplies were used to measure only the LDC0851 current consumption. The first supply was a regular bench power supply that powered the majority of the board (including the MSP430). The second power supply was the power analyzer that only powered the LDC0851. Both of these supplies were connected so that they were referenced from the same place (the negative power supply terminals of both supplies were connected together).

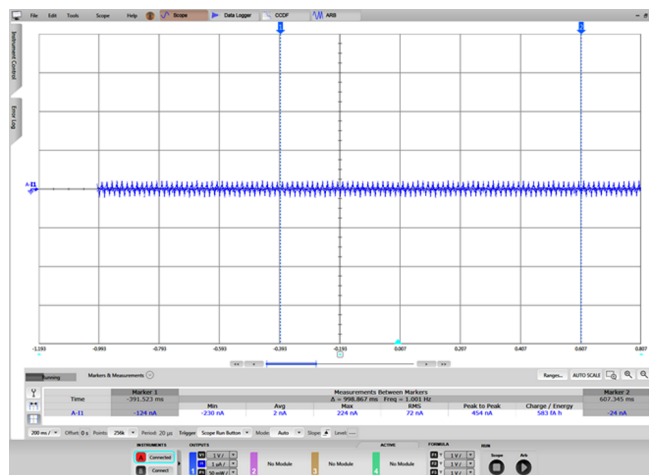
The test was performed when the case was fully closed, which corresponds to the maximum current for this design. Based on the power provided to the LDC0851 from the power analyzer, the power analyzer plots the average current consumption of the LDC0851.

Two readings using different ranges were taken to properly use this equipment for sensing the average current consumption. One reading was taken when the LDC0851 was enabled (peak current in the mA range) and another reading was taken when the LDC0851 was disabled (peak current in the nA range). The LDC0851 was sampled at a rate of 1 Hz; so, for each second the LDC0851 was only enabled long enough for one valid reading and then turned OFF for the remainder of the second duration.

 [50](#) and  [51](#) show the resulting plots obtained from the power analyzer when the LDC0851 was enabled and when it was disabled, respectively, for the one-sense-coil variant of this design.



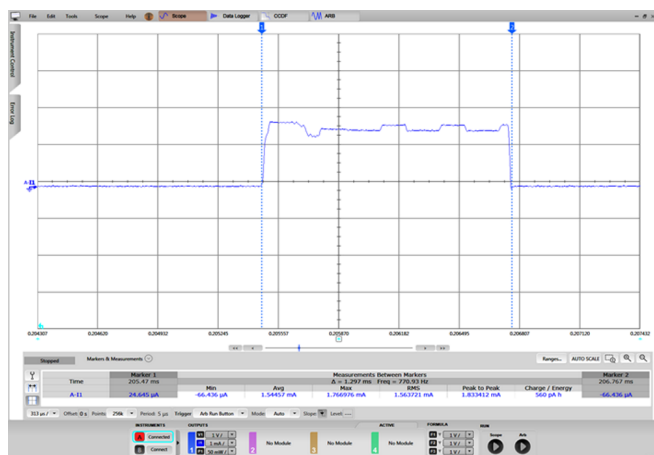
☒ 50. Average Current Consumption: LDC0851 Enabled, One-Sense-Coil Implementation



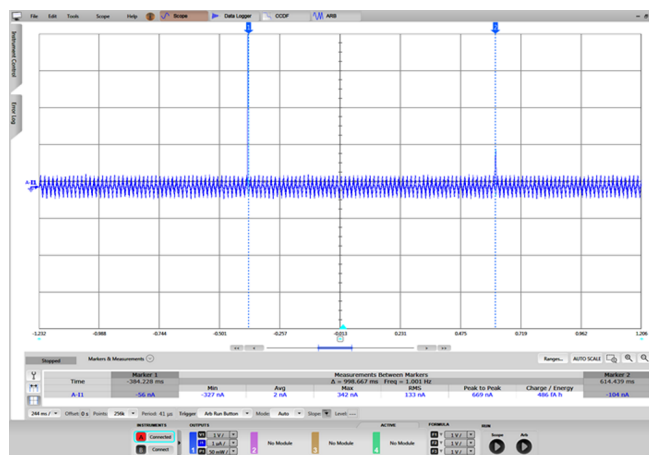
☒ 51. Average Current Consumption: LDC0851 Disabled, One-Sense-Coil Implementation

In ☒ 50, the average current consumption when the LDC0851 was enabled was 1.723 mA for a duration of 1.06 ms. For the rest of the 998.94 ms, the LDC0851 was disabled with an average current consumption of 2 nA, as shown in ☒ 51. By averaging these current consumptions over time, the LDC0851 average current consumption is calculated to be equal to:  
 $((1723) \times (1.06) + (0.002) \times (998.94)) / 1000 = 1.83 \mu\text{A}$ , which is less than 2  $\mu\text{A}$ .

The same test was performed for the two-sense-coil variant of this board. ☒ 52 and ☒ 53 show the resulting measurements for this two-sense-coil variant.



☒ 52. Average Current Consumption: LDC0851 Enabled, Two-Sense-Coil Implementation



☒ 53. Average Current Consumption: LDC0851 Disabled, Two-Sense-Coil Implementation

In ☒ 52, the average current consumption when the LDC0851 was enabled was 1.545 mA for a duration of 1.297 ms. For the rest of the 998.703 ms, the LDC0851 was disabled with an average current consumption of 2 nA, as shown in ☒ 53. By averaging these current consumptions over time, the LDC0851 average current consumption is calculated to be equal to:  
 $((1545) \times (1.297) + (0.002) \times (998.703)) / 1000 = 2.01 \mu\text{A}$ .

## 6 Design Files

### 6.1 Schematics

To download the schematics, see the design files at [TIDA-01377](#).

### 6.2 Bill of Materials

To download the bill of materials (BOM), see the design files at [TIDA-01377](#).

### 6.3 PCB Layout Recommendations

To view PCB layout recommendations, see [3.3.4.1.2](#).

### 6.4 CAD Project

To download the CAD project files, see the design files at [TIDA-01377](#).

### 6.5 Gerber Files

To download the Gerber files, see the design files at [TIDA-01377](#).

## 7 Software Files

To download the software files, see the design files at [TIDA-01377](#).

## 8 Related Documentation

1. Texas Instruments, [Magnetic Tamper Detection Using Low-Power Hall Effect Sensors](#), TIDA-00839 Reference Design (TIDUB69)
2. Texas Instruments, [LDC0851 Quick-Start Guide](#), LDC0851 Application Report (SNOA947)
3. Texas Instruments, [Inductive sensing: Are narrow-band LC sensors immune to DC magnetic fields?](#), E2E™ Online Community Forum ([https://e2e.ti.com/blogs\\_/b/analogwire/archive/2016/03/14/inductive-sensing-are-narrow-band-lc-sensors-immune-to-dc-magnetic-fields](https://e2e.ti.com/blogs_/b/analogwire/archive/2016/03/14/inductive-sensing-are-narrow-band-lc-sensors-immune-to-dc-magnetic-fields))
4. Texas Instruments, [LDC Target Design](#), LDC0851 Application Report (SNOA957)

### 8.1 商標

MSP430, E2E are trademarks of Texas Instruments.

IAR is a trademark of IAR Systems AB.

すべての商標および登録商標はそれぞれの所有者に帰属します。

## 9 About the Author

**MEKRE MESGANAW** is a systems engineer in the Grid Infrastructure group at Texas Instruments, where he primarily works on grid monitoring and electricity metering customer support and reference design development. Mekre received his Bachelor of Science and Master of Science in computer engineering from the Georgia Institute of Technology.

## TIの設計情報およびリソースに関する重要な注意事項

Texas Instruments Incorporated ("TI")の技術、アプリケーションその他設計に関する助言、サービスまたは情報は、TI製品を組み込んだアプリケーションを開発する設計者に役立つことを目的として提供するものです。これにはリファレンス設計や、評価モジュールに関係する資料が含まれますが、これらに限られません。以下、これらを総称して「TIリソース」と呼びます。いかなる方法であっても、TIリソースのいずれかをダウンロード、アクセス、または使用した場合、お客様(個人、または会社を代表している場合にはお客様の会社)は、これらのリソースをここに記載された目的にのみ使用し、この注意事項の条項に従うことに同意したものとします。

TIによるTIリソースの提供は、TI製品に対する該当の発行済み保証事項または免責事項を拡張またはいかなる形でも変更するものではなく、これらのTIリソースを提供することによって、TIにはいかなる追加義務も責任も発生しないものとします。TIは、自社のTIリソースに訂正、拡張、改良、およびその他の変更を加える権利を留保します。

お客様は、自らのアプリケーションの設計において、ご自身が独自に分析、評価、判断を行う責任がお客様にあり、お客様のアプリケーション(および、お客様のアプリケーションに使用されるすべてのTI製品)の安全性、および該当するすべての規制、法、その他適用される要件への遵守を保証するすべての責任をお客様のみが負うことを理解し、合意するものとします。お客様は、自身のアプリケーションに関して、(1) 故障による危険な結果を予測し、(2) 障害とその結果を監視し、および、(3) 損害を引き起こす障害の可能性を減らし、適切な対策を行う目的での、安全策を開発し実装するために必要な、すべての技術を保持していることを表明するものとします。お客様は、TI製品を含むアプリケーションを使用または配布する前に、それらのアプリケーション、およびアプリケーションに使用されているTI製品の機能性を完全にテストすることに合意するものとします。TIは、特定のTIリソース用に発行されたドキュメントで明示的に記載されているもの以外のテストを実行していません。

お客様は、個別のTIリソースにつき、当該TIリソースに記載されているTI製品を含むアプリケーションの開発に関連する目的でのみ、使用、コピー、変更することが許可されています。明示的または黙示的を問わず、禁反言の法理その他どのような理由でも、他のTIの知的所有権に対するその他のライセンスは付与されません。また、TIまたは他のいかなる第三者のテクノロジーまたは知的所有権についても、いかなるライセンスも付与されるものではありません。付与されないものには、TI製品またはサービスが使用される組み合わせ、機械、プロセスに関連する特許権、著作権、回路配置利用権、その他の知的所有権が含まれますが、これらに限られません。第三者の製品やサービスに関する、またはそれらを参照する情報は、そのような製品またはサービスを利用するライセンスを構成するものではなく、それらに対する保証または推奨を意味するものでもありません。TIリソースを使用するため、第三者の特許または他の知的所有権に基づく第三者からのライセンス、あるいはTIの特許または他の知的所有権に基づくTIからのライセンスが必要な場合があります。

TIのリソースは、それに含まれるあらゆる欠陥も含めて、「現状のまま」提供されます。TIは、TIリソースまたはその仕様に関して、明示的か暗黙的にかかわらず、他のいかなる保証または表明も行いません。これには、正確性または完全性、権原、続発性の障害に関する保証、および商品性、特定目的への適合性、第三者の知的所有権の非侵害に対する黙示の保証が含まれますが、これらに限られません。

TIは、いかなる苦情に対しても、お客様への弁済または補償を行う義務はなく、行わないものとします。これには、任意の製品の組み合わせに関連する、またはそれらに基づく侵害の請求も含まれますが、これらに限られず、またその事実についてTIリソースまたは他の場所に記載されているか否かを問わないものとします。いかなる場合も、TIリソースまたはその使用に関連して、またはそれらにより発生した、実際の、直接的、特別、付随的、間接的、懲罰的、偶発的、または、結果的な損害について、そのような損害の可能性についてTIが知らされていたかどうかにかかわらず、TIは責任を負わないものとします。

お客様は、この注意事項の条件および条項に従わなかったために発生した、いかなる損害、コスト、損失、責任からも、TIおよびその代表者を完全に免責するものとします。

この注意事項はTIリソースに適用されます。特定の種類の資料、TI製品、およびサービスの使用および購入については、追加条項が適用されます。これには、半導体製品(<http://www.ti.com/sc/docs/stdterms.htm>)、評価モジュール、およびサンプル(<http://www.ti.com/sc/docs/sampterms.htm>)についてのTIの標準条項が含まれますが、これらに限られません。